UC-25
LBL-18599
c1

Lawrence Berkeley Laboratory
UNIVERSITY OF CALIFORNIA

Materials & Molecular Research Division

RECEIVED
LAWRENCE
BERKELEY LABORATORY
FEB 11 1985
LIBRARY AND
DOCUMENTS SECTION

EFFECTS OF ION BOMBARDMENT ON THE MORPHOLOGY OF LEAD FILMS

M.J. Armstrong* and R.H. Muller
(*M.S. Thesis)

December 1984

For Reference
Not to be taken from this room

LBL-18599
c.1

Prepared for the U.S. Department of Energy under Contract DE-AC03-76SF00098

DISCLAIMER

This document was prepared as an account of work sponsored by the United States Government. While this document is believed to contain correct information, neither the United States Government nor any agency thereof, nor the Regents of the University of California, nor any of their employees, makes any warranty, express or implied, or assumes any legal responsibility for the accuracy, completeness, or usefulness of any information, apparatus, product, or process disclosed, or represents that its use would not infringe privately owned rights. Reference herein to any specific commercial product, process, or service by its trade name, trademark, manufacturer, or otherwise, does not necessarily constitute or imply its endorsement, recommendation, or favoring by the United States Government or any agency thereof, or the Regents of the University of California. The views and opinions of authors expressed herein do not necessarily state or reflect those of the United States Government or any agency thereof or the Regents of the University of California.

LBL-18599

EFFECTS OF ION BOMBARDMENT ON THE MORPHOLOGY OF LEAD FILMS

Michael Jefferey Armstrong
with Rolf H. Muller

Lawrence Berkeley Laboratory
Chemical Engineering Department
University of California
Berkeley, California 94720

This work was done with support from the Department of Energy
under Contract No. DE-AC03-76SF00098

Table of Contents

List of Figures v

List of Tables ix

Abstract xi

1. Introduction 1

2. Experimental Apparatus and Procedure 7

   2.1. Sample Preparation 7

   2.2. Vacuum Techniques 9

   2.3. Ellipsometry 15

3. Optical Model 21

4. Results and Discussion 27

   4.1. Refractive Index of Copper and Lead 27

   4.2. Pit Formation in Lead Films 30

5. Conclusion 46

Acknowledgments 47

6. APPENDIX A. Auger Electron Spectroscopy 48

7. APPENDIX B. Ellipsometry 52

8. APPENDIX C. Program 4ZONE 56

9. References 85

List of Figures

1) Schematic of the evaporator attached to the ultrahigh vacuum chamber.

2) Ultrahigh vacuum chamber for Auger electron spectroscopy and ion bombardment. View ports allow ellipsometry of samples in the chamber.

3) Schematic of Retarding Field Analyzer (RFA).

4) Block Diagram of Electronics Used with the retarding field analyzer for Auger electron analysis.

5) Electron current energy distribution as collected by the retarding field analyzer: The sample consists of an island lead film upon a copper substrate. The retarding field voltage is ramped at 100 V/min from 30 to 1700 V. A 12 V peak-to-peak modulation of 1000 Hz is superimposed upon the retarding field. The excitation energy is 1500 eV. (a) Electron current collected with energy above the retarding field potential (2nd grid potential), (b) electron current (N(e)) of the specified energy (first derivative of fig. a), (c) Derivative of electron current of the specified energy (second derivative of fig. a).

6) Block diagram of the optical components of the spectroscopic ellipsometer with a polarizer-compensator-analyzer (PCA) configuration.

7) Diagram of island and pitted films. a) Island film, continuous substrate surface, b) Pitted film, continuous film covered surface.

8) Schematic of model surfaces used for interpreting spectroscopic ellipsometry measurments.

9) Spectral Dependence of the refractive index of bulk copper following 60 min of 1100 eV Ar ion bombardment at a 75° angle of incidence. literature values for clean surface [refs. 29,30]. a) Refractive Index, b) Extinction Coefficient.

10) Spectral ellipsometric measurements from four separate copper samples following ion bombardment with 1100 eV Ar ions. The measurments were taken at sputter times greater than that required to reach steady optical properties of the surface. a) Delta, b) Psi.

11) Spectral dependence of the refractive index of vapor deposited lead following 10 min. of 1100 eV Ar ion bombardment. The ion beam intersected the surface at an angle of incidence of 75°. Literature values (●) are shown for comparison from Lijenvall, Mathewson, and Myers [ref. 36]. a) Refractive Index, b) Extinction Coefficient.

12) Spectral ellipsometric measurements from a electrochemical lead deposit of 0.039 C/cm^2 (340 Å) intermittently through out 125 min of 1100 eV Ar ion bombardment. The changes in the optical properties reflect the removal of oxide for the first 15 min and the generation of pits throughout the 125 min of sputtering. The spectral scan after 125 min of ion bombardment is that of bare copper. The Angle of incidence of the ion beam is 75°. a) Delta, b) Psi.

13) Comparison of the measured delta and psi to the calculated values for the 0.039 C/cm^2 (369 Å compact) lead deposit following 35 min. of ion bombardment. The optical model consist of a a 0.74 cover-

age of lead islands with an underlying 30 Å lead film. Both the islands and continuous film have a porosity of 0.2. The substrate is bulk copper. a) Delta b) Psi.

14) Fraction of the copper surface covered by lead as a function of sputter duration for a 0.039 C/cm^2 (369 Å compact) electrochemical deposit of lead. The coverage is determined with Auger electron spectroscopy and spectroscopic ellipsometry. The ion source consisted of 1100 eV Ar ions with an angle of incidence on the sample surface of 75°.

15) Scanning electron micrograph of a electrochemical lead deposit of 0.079 C/cm^2 (738 Å compact) following 65 min of 1.1 keV Ar ion bombardment at an angle of incidence of 75°. The micrograph shows severe pitting of the lead film. The pits are on the order of 1 μm across and penetrate into the underlying copper substrate.

16) Scanning electron micrograph of a Pb vapor deposit made with a VARIAN evaporator under a background pressure of 10-4 torr. A 1 μm polishing paste was used on the copper substrate rather than the 0.05 μm polish used on the substrate of the ion bombarded deposits. No pits are present.

17) Scanning electron micrograph of a Pb Vapor deposit after 45 min of 1 keV Ar ion bombardment. Spectroscopic ellipsometry measurments fitted with a coherent superposition model of the pits indicates a 68% coverage of the copper surface by lead of 20% porosity with a thickness greater than 450 Å. The photo shows severe pitting similar to that in fig. 15.

18) Scanning electron micrograph of a vapor deposit of lead formed in the ultrahigh vacuum chamber with a background pressure of 10^{-7} torr following 10 min of 1.1 keV Ar ion bombardment. Interpretation of the optical measurements with a compact film model indicated an initial thickness of 100 Å before ion bombardment. No oxide was indicated. Pitting similar to that of figs. 15 and 17 is present with pit diameters of about 1000 Å.

19) Scanning electron micrograph of a vapor deposit of lead formed in the ultrahigh vacuum chamber with a background pressure of 10^{-7} torr following 65 min of 1.1 keV Ar ion bombardment. The film was thicker than 300 Å and did not have an oxide layer before ion bombardment. Pitting similar to that in fig. 15 and 17 is shown.

20) Comparison of the island coverage with the carbon AES peak height as a function of the ion bombardment duration for the 0.039 C/cm^2 (369 Å compact) lead deposit.

21) Universal escape depth curve for electrons [ref. 31].

22) Schematic of a KLL Auger electron emission.

23) Electric wave component of an electromagnetic wave decomposed into two orthogonal components s and p.

List of Tables

1) Sputtering yields of carbon, copper, and lead. a) Sputtering yield for copper and carbon with 0.5, 1.0, and 10 keV He, Ne, Ar, Kr, and Xe ions [ref. 4]. b) Sputtering rate for carbon, copper and lead using 0.5 keV Ar ions at normal incidence at a current density of 1 mA/cm^2 [ref. 13].

2) Optical model parameters for the ion bombardment of a electrochemically deposited lead sample of 0.039 C/cm^2 (369Å compact). The deposit was made in the presence of Rhodamine-b chloride in a sodium perchorate supporting electrolyte. The Optical model parameters are tabulated as a function of ion bombardment duration of 1100 eV Ar ions. The optical model consist of either an lead-oxide or porous-lead-island film upon a porous lead film with a copper substrate.

3) Fraction of copper substrate covered with lead as a function of ion bombardment duration of 1100 eV Ar ions for a electrochemically deposited lead sample of 0.039 C/cm^2 (369 Å compact). The surface coverage was determined from optical modeling of the optical properties and from Auger electron spectroscopy.

4) Derivation of psi and delta from azimuths of the polarizer, quarter wave retarder, and analyzer [ref. 22].

EFFECTS OF ION BOMBARDMENT ON THE MORPHOLOGY OF LEAD FILMS

Michael Jefferey Armstrong
with Rolf H. Muller

Lawrence Berkeley Laboratory
Department of Chemical Engineering
University of California
Berkeley, California 94720

Abstract

The effects of ion bombardment on the morphology of compact lead films were investigated with spectroscopic ellipsometry, Auger electron spectroscopy (AES), and scanning electron microscopy. Lead films of under 100 nm in thickness were prepared by electrodeposition and vacuum-vapor deposition. In contrast to the expected uniform removal of the surface by ion bombardment, assumed in the determination of composition by AES, a nonuniform removal of the surface has been found to occur resulting in pitting or island formation. This pitting is independent of the mode of formation of the film and the presence of an oxide overlayer. An optical model of a film distributed as islands was used to interpret spectroscopic ellipsometry measurements. The model was based on the coherent superposition of polarization states resulting from reflection on the bare and film-covered surfaces. Scanning electron micrographs confirmed the use of the island model for the surface morphology. The surface coverage of lead calculated from spectroscopic ellipsometry agrees well with the results of Auger electron spectroscopy measurements.

1. Introduction

The original purpose of this research was to gain information on the effect of organic adsorbates on the initial stage of electrolytic metal deposition. This research was to expand on the results of J.C. Farmer and R. Muller [refs. 1,2] for the electrolytic deposition of lead in the presence of Rhodamine-B chloride. Their investigation demonstrated a reduction of porosity of lead films deposited in the presence of Rhodamine-B as compared to deposits without Rhodamine-B. Auger Electron Spectroscopy (AES) and spectroscopic ellipsometry were to be used in conjunction with ion bombardment to determine the porosity and composition profiles of the lead deposits. The uniform removal of surface atoms by ion bombardment was needed to profile the lead films. However, severe morphology changes of the lead film have been found due to ion bombardment.

Therefore the objectives of this research have been changed to:

(1) Investigate the effects of ion bombardment on the morphology of thin lead films

(2) Investigate the validity of a coherent super-position model used previously for the interpretations of measurements of a surface covered with an island film. Spectroscopic ellipsometry and AES were used to determine the changes occurring on thin lead films with ion bombardment.

Morphological and compositional changes of a surface induced by ion bombardment are important when ion bombardment is used in conjunction with any surface analysis techniques. Ion bombardment can be used to

etch surfaces for depth analysis by techniques such as AES. Apart from thinning, the undesirable effects of ion bombardment on a film include surface roughening, preferential sputtering, and recoil implantation [ref. 3,4].

Roughness reduces the depth resolution of surface analyses techniques such as AES since the surface is sampled at various depths. Ion bombardment results in the increase in surface roughness. Several factors such as impurities, pre-existing roughness, angular dependence of etch rate, and crystal-face dependence of etch rate affect the evolution of surface roughness.

The evolution of surface roughness can be the result of impurities on the surface [ref. 5,6]. Ion bombardment of gold with a small amount of chromium caused the formation of cones several micrometers high [ref. 4]. Ion bombardment of <111> Pb single crystals showed the formation of cones due to a carbon contamination [ref. 35]. The cones were formed because of contaminants which protected underlying sections of the surfaces. Surface migration enables surface species to concentrate on local areas of the surface. If there is a difference in the sputter rates between the locally concentrated species and the remainder of the surface, there will be an increase in the surface roughness due to preferential sputtering.

The presence of roughness before ion bombardment, contributes to further generation of roughness. Kelly and Auciello [ref. 7] found that pre-existing asperites on an impurity-free copper surface formed into cones when the surface was bombarded with 12-keV Kr^+ atoms at normal incidence. These cones were found to be unstable and were removed by

extended sputtering.

The angular dependence of etch rate results in topographical changes. Ripples were formed on Si and pits were formed on Cu when ion bombarded by 9 keV Kr^+ ions at an angle of incidence of 50° from the normal of the surface [ref. 8]. The ripples on the Si substrate formed a leading face normal to the incident ion beam and a trailing face parallel to the incident ion beam. The orientation of the ripple face was a result of a maximum sputter rate occurring on surfaces normal to the ion beam and a negligible sputter rate on faces parallel to the ion beam. The dependence of sputter rate on the angle at which the ion impinges on the surface contributed to the roughening of the surface by creating faces with a preferred orientation. The degree of pit formation on a <11,3,1> copper surface was found to vary with the azimuthal direction at the same angle of incidence. The dependence of pit formation on azimuthal direction was attributed to the alignment of the ion beam with dislocation axes or planes. The effects of angular preference can be reduced by rotating the sample during ion bombardment [ref. 9].

The accuracy of a composition profile is affected by differences in the sputter yields of the different elements of a multicomponent sample [refs. 10,11,12]. The surface composition is altered by the rate at which different elements are etched. Elements that are difficult to sputter are concentrated on the surface during the ion bombardment. Data are available for the relative sputter yields of some elements and compounds [refs. 4,13]. Table 1 gives some values of sputter rates for several elements and compounds for various ion energies and ion species.

Table 1. Sputtering yields of carbon, copper, and lead. (a) Sputtering yield for copper and carbon with 0.5, 1.0, and 10 keV He, Ne, Ar, Kr, and Xe ions [ref. 4]. (b) Sputtering rate for carbon, copper and lead using 0.5 keV Ar ions at normal incidence at a current density of 1 mA/cm/cm [ref. 13].

1a [ref 4]

		Sputtering Yield (atoms/ion)				
Ion energy (keV)	Material	He	Ne	Ar	Kr	Xe
0.5	Cu	0.24	1.8	2.4	2.4	2.1
0.5	C	0.7		0.12	0.13	0.17
1	Cu		2.7	3.6	3.6	3.2
10	Cu		3.2	6.6	8	10

1b [ref 13]

Sputtering Rate For 0.5 keV Ar Ions, Normal incedence, 1 mA/cm^2	
Material	Sputter rate (Å/min)
C	50
Cu	650
Pb	3000

Recoil implantation occurs when a atom is knocked into the substrate instead of off the surface by ion bombardment. Recoil implantation affects accuracy of the composition profile by creating a layer of mixed composition [refs. 10,12]. A small fraction of the ion-beam energy is used in the removal of surface atoms [ref. 4]. Some of the remaining energy is retained in backscattered ions, but most of the energy is dissipated in moving the surface molecules around, on, and into the

surface. Ion energy, angle of incidence, mass ratio of ions to surface species, and diffusional properties affect the degree of mixing [ref. 14]. Low ion energy, oblique angles of incidence, and low mass ratio of ions to surface species reduce the effects of recoil implantation [ref. 4]. Anderson [ref. 15] calculated the cascade mixing effects on depth resolution at steady state for a range of elements under 1 to 10 keV Argon ion bombardment.

A few studies have been performed on the effects of ion bombardment on the optical properties of surfaces. These studies are described briefly below.

Aspnes and Studna [ref. 16] investigated <111> germanium surfaces bombarded with low-energy (200-1000 eV) ions before and after annealing. They used spectroscopic ellipsometry, Auger electron analysis, and low energy electron diffraction (LEED). The ion bombarded surface was modeled as a layer of damaged material on the germanium crystal surface. Repeated cycles of ion bombardment and annealing produced a macroscopic scattering of light but did not cause changes of ellipsometric data. The scattered light was attributed to slip planes and thermal etch pits that deflected the light out of the specular beam path and did not influence the ellipsometric data. The density of the damaged layer was determined to be 5.0 g/cm^3, compared to 5.37 g/cm^3 for the Ge crystal. The Bruggeman effective-medium approximation was used to determine the density of the damaged layer from the measured dielectric function. The thickness of the damaged layer was calculated for several bombardment energies and was found to be proportional to the ion energy to the two-thirds power. For surfaces bombarded by argon ions, the measured damage depth varied

from 25 Å at an ion energy of 200 eV to 80 Å at an ion energy of 1000 eV.

Ibrahim and Bashara [ref. 17] studied the effects of bombardment by argon ions on the optical properties of silicon. Ellipsometry measurements at multiple angles of incidence were used to determine the optical properties of the damaged layer. The refractive index of the damaged layer was found to be 3.91-0.22i at a wavelength of 6328 Å compared to 3.90-0.02i for the silicon substrate at the same wavelength. The authors used a two-layer film model to interpret the results, consisting of a thin oxide film (4 Å) with the damaged layer underneath. The substrate was undamaged silicon. They assumed that the defect-density was small enough that changes in psi could be related linearly to defect-density. Using this linear relationship, they found that the defect-density was a nonlinear function of the bombardment energy for argon ions with energies from 150 to 400 eV.

Both Ibrahim and Bashara and Aspnes and Studna attribute the change in the optical properties of the ion-bombarded surfaces to the decrease in density or increase in microporosity of a damaged layer on the crystal surfaces. The porosity is attributed to defects or displaced atoms in the damaged layer. Roughness may also lead to the same optical properties as a damaged layer that contains defects and displaced atoms.

2. Experimental Apparatus and Procedure

2.1. Sample Preparation

The lead films used in this study were deposited by electrochemical and evaporation methods. These methods produced films that covered the surface uniformly. Oxygen-free copper was used as a substrate with both methods of deposition.

The transfer of the samples to the UHV chamber was performed in a nitrogen atmosphere with a Huntington mechanical feedthrough. The mechanical feedthrough was manipulated by a magnetic coupling. Following the placement of the sample within the feedthrough, the feedthrough valve was closed. The sample-transfer tube was evacuated for 30 minutes reaching a pressure of 10^{-7} torr before the lead deposit was placed into the vacuum chamber. After positioning the sample for AES and ellipsometry in the UHV chamber, the chamber pressure was reduced to 10^{-8} torr.

The copper substrates were 12.7 mm in diameter. The chosen diameter was compatible with the clearance in the UHV sample-transfer tube. The substrates were polished mechanically. Copper electrodes were mounted in a 25.4 mm dia. copper holder for polishing. The holder reduced the surface curvature which resulted from polishing. The electrode was sanded flat in the holder with 600 grit emery paper on a glass plate. Each step of the mechanical polishing involving either a change in sandpaper grit size or polishing-paste size was preceded with a period of ultrasonic cleaning in a LABTONE soap solution. Sanding by emery paper was followed with 1 micron diamond paste in a lapping oil extender on a

canvas-covered rotating surface. Final polishing was done with 0.05 μm Alumina powder in a water extender on a MICROMET MICROCLOTH felt surface.

A thin-film electrochemical-cell configuration was used for electrodeposition. A lead-counter electrode was placed approximately 2 mm from, and parallel to, a copper cathode. The cell voltages were monitored with an Ag/AgCl reference electrode located in a separate reservoir of electrolyte which was connected to the cell by teflon spaghetti tubing. The thin-cell apparatus was located within a glove bag filled with nitrogen.

An electrolyte consisting of 1.0M $NaClO_4$, 0.005M $Pb(NO_3)_2$, and 10^{-5} M rhodamine-B chloride at a pH of 2.4 was used in the depositions. This electrolyte remained in contact with the copper electrode for 60 minutes before any electrolysis was performed. The 60-minute delay between addition of the electrolyte and the electrolysis was necessary for the rhodamine-B dye to adsorb on the copper surface [refs. 1,2]. The electrochemical deposition of lead was performed potentiostatically at -700 mV relative to a Ag/AgCl reference electrode. Films of -0.078 and -0.039 C/cm^2 were deposited. These films corresponded to a compact lead deposit of 738 and 369 Å as based on the density of bulk lead. After deposition, the samples were rinsed quickly in distilled water with excess water removed by compressed freon.

Vapor deposition of lead films were performed under vacuum, both in the UHV vacuum chamber and in a VARIAN evaporator. Both depositions were made by vaporizing high purity lead (99.999%) from a tungsten basket. The tungsten acted as both a container and as a heating element.

The background pressure in the VARIAN apparatus was 10^{-4} torr. The tungsten basket was located approximately 5 cm from the sample. To ensure that the film would deposit evenly, the sample was rotated during vaporization of the lead. The vapor deposits were exposed to atmospheric air for approximately 10 min during the transfer from the vapor coater to the UHV chamber.

Vapor deposits without exposure to air were made within an attachment to the UHV chamber used for ion bombardment and AES (fig. 1). The sample transfer tube was used to position the sample underneath the vapor depositer. The tungsten basket of the vapor depositor was located 5 cm above the sample. Vapor deposits were made in a background pressure of 10^{-7} torr after a purge with nitrogen.

2.2. Vacuum Techniques

Ion sputtering and AES are ultrahigh vacuum (UHV) techniques. A UHV chamber with view ports for ellipsometry was used for both ion bombardment and AES (fig. 2). The view ports were positioned for a 75° angle of incidence of the light source used for ellipsometry. The electron gun for AES and the ion gun for ion bombardment were mounted at a 75° angle of incidence but at different azimuthal positions. The electron gun and ion gun were positioned at 30° and 60° respectively from the plane of incidence of the ellipsometer.

A Varian 3-KeV ion gun was used for sputter etching. Ion sputtering was performed with argon ions at an energy of 1100 eV in a background pressure of $5.0 * 10^{-5}$ torr. The etch-rate was measured from changes in the film thickness with the amount of sputter time. The thickness was

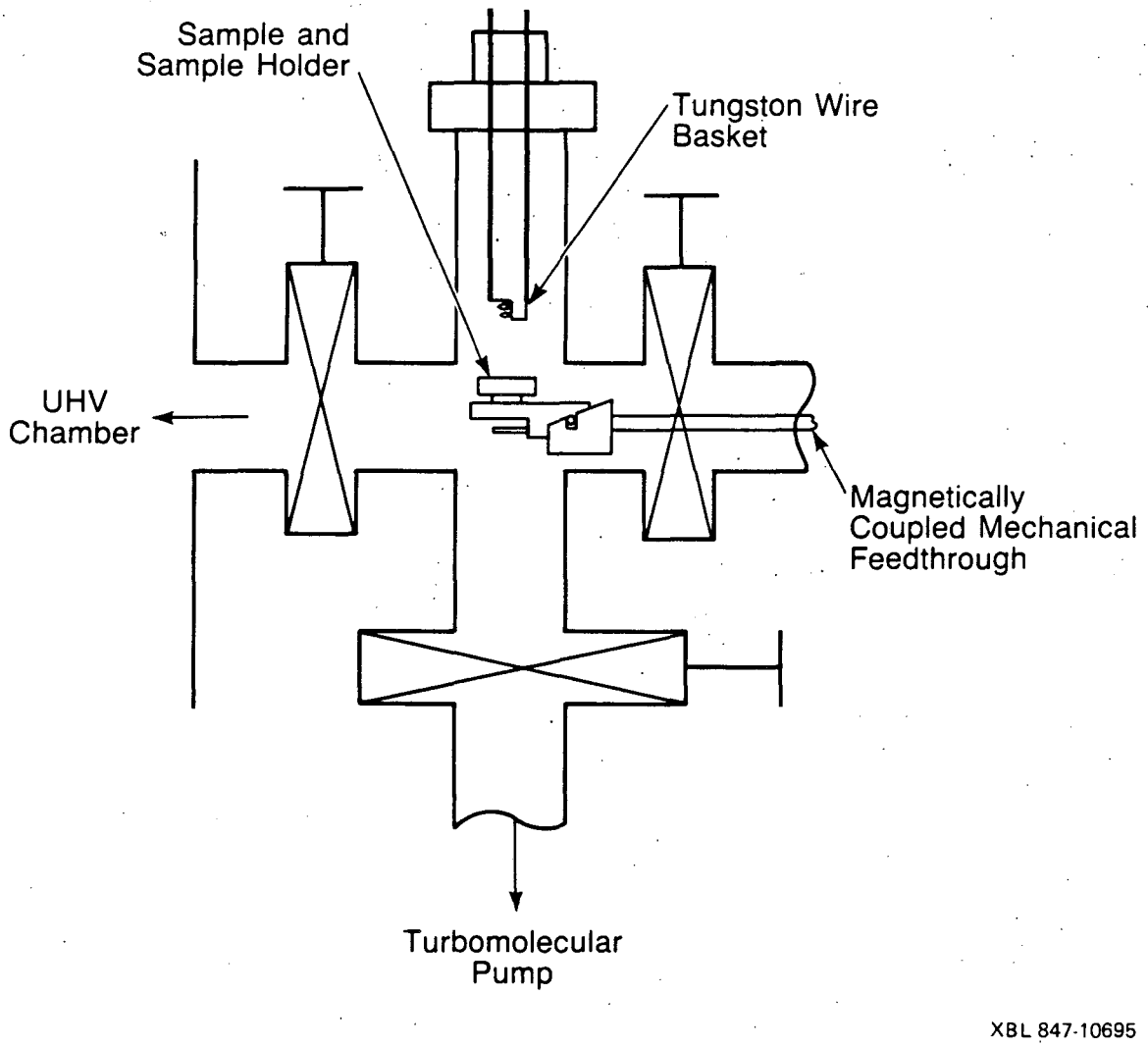

Fig. 1. Schematic of the evaporator attached to the ultrahigh vacuum chamber.

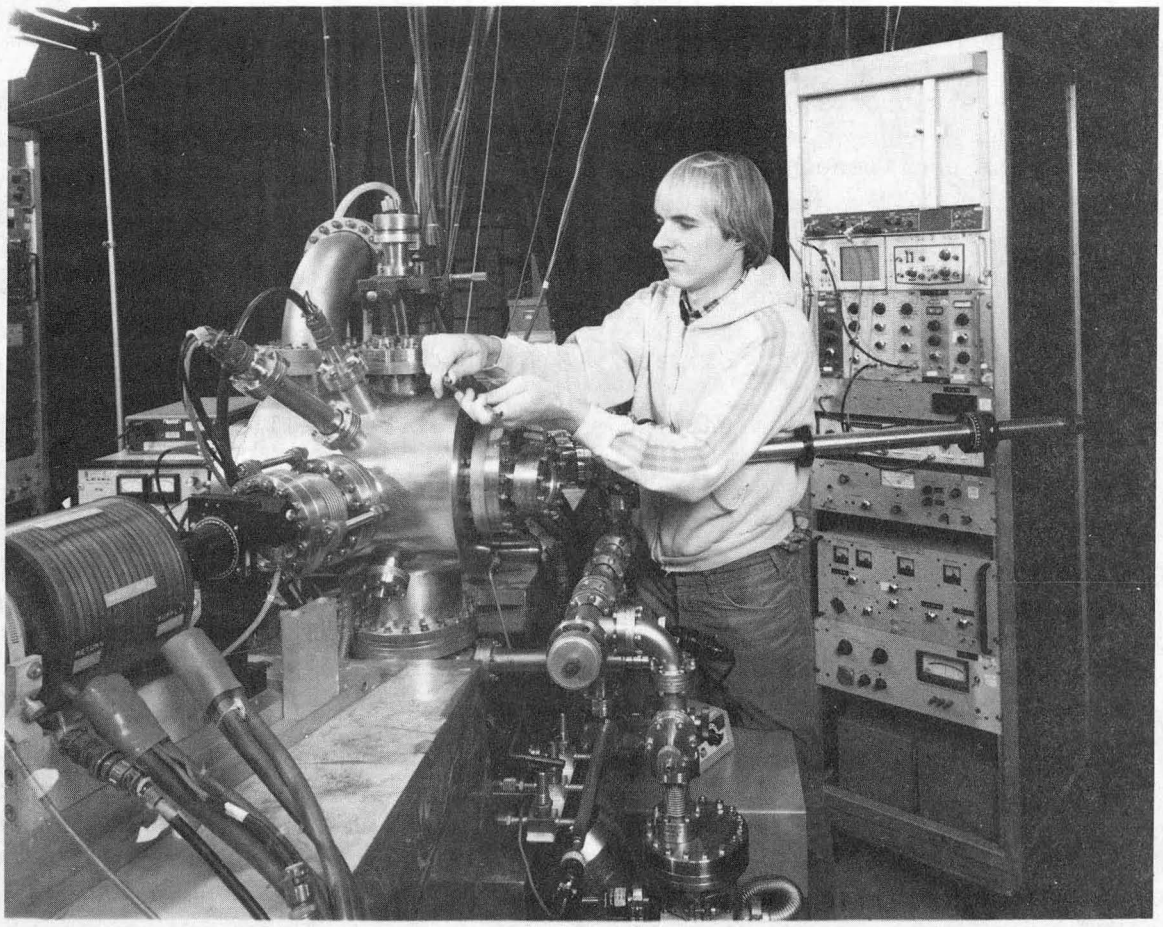

CBB 820-10883

Fig. 2. Ultrahigh vacuum chamber for auger electron spectroscopy and ion bombardment. View ports allow ellipsometry of samples in the chamber.

determined from spectroscopic ellipsometric measurements. The ion beam was rastered across the sample surface to obtain an even bombardment of the surface.

The electron source for AES was a modified oscilloscope electron gun. The oscilloscope gun filament was replaced by a Varian filament of higher emission capabilities. Auger electron transitions from the surface of the sample were induced by a 1500-eV electron beam. The electron beam was focused to approximately 3 mm in diameter at the position of the sample. The beam sampled a 3 mm by 12.5 mm elliptical area on the surface.

A retarding field analyzer (RFA) was used for the determination of the distribution of the electron current with respect to electron energy (figs. 3,4) [refs. 18,19]. The RFA consisted of three grids and a phosphorus screen. The first and third grids were grounded; the second grid was biased to a negative potential between 0 and 1500 V. The phosphorus screen was charged to +100 V and acted as the electron collector. The electron current collected by the phosphorus screen was amplified and processed through a phase-sensitive detector (lock-in amplifier).

Electrostatic repulsion with the RFA was used to determine the energy distribution of the emitted electrons. The electrons with energies higher than the voltage of the second grid were collected on the phosphorous screen. Electrons with less energy are electrostatically repelled. A 1000-Hz modulation was imposed on the potential of the second grid. The second grid potential was modulated 4 V peak-to-peak for analysis of the Auger electrons with energies less than 100 eV. A modulation of 10 V peak-to-peak was used for Auger electron energies

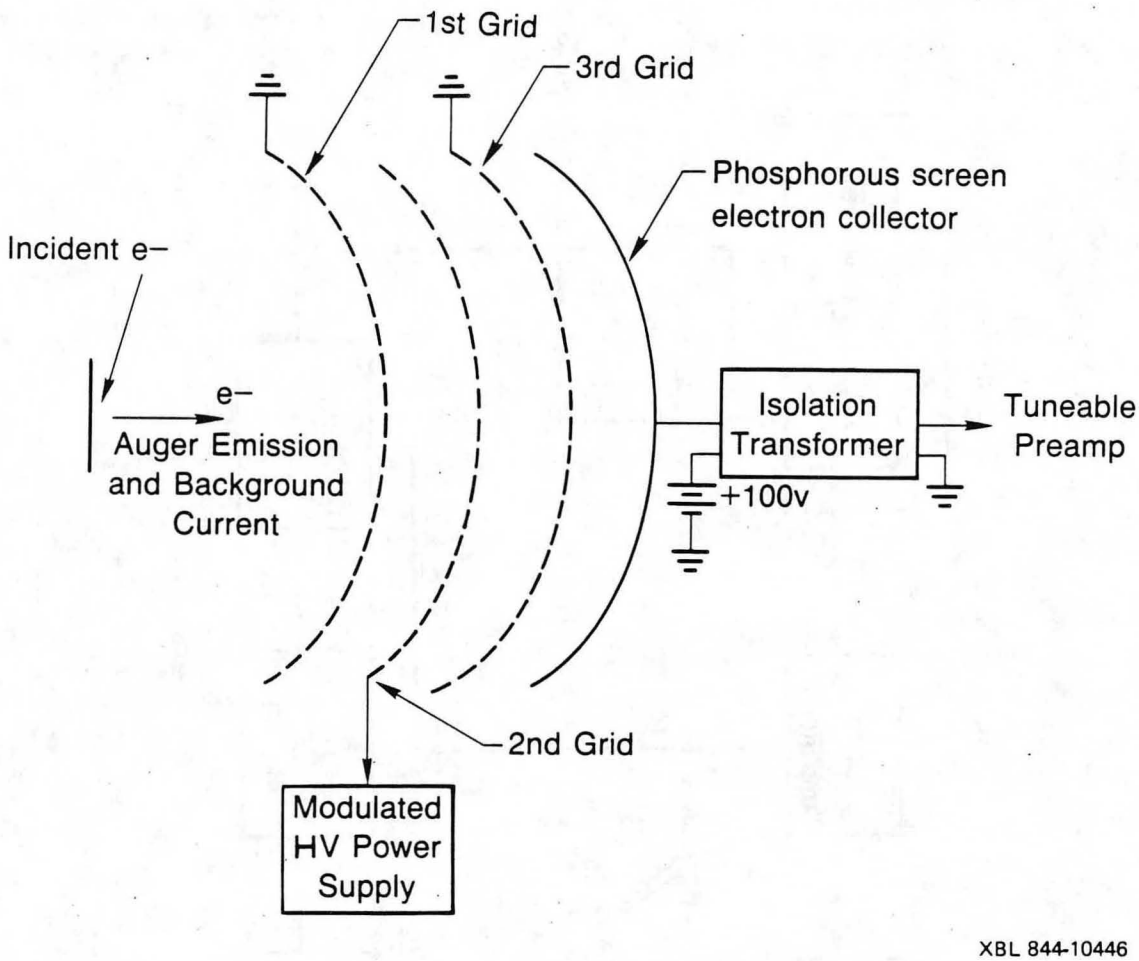

Fig. 3. Schematic of retarding field analyzer (RFA).

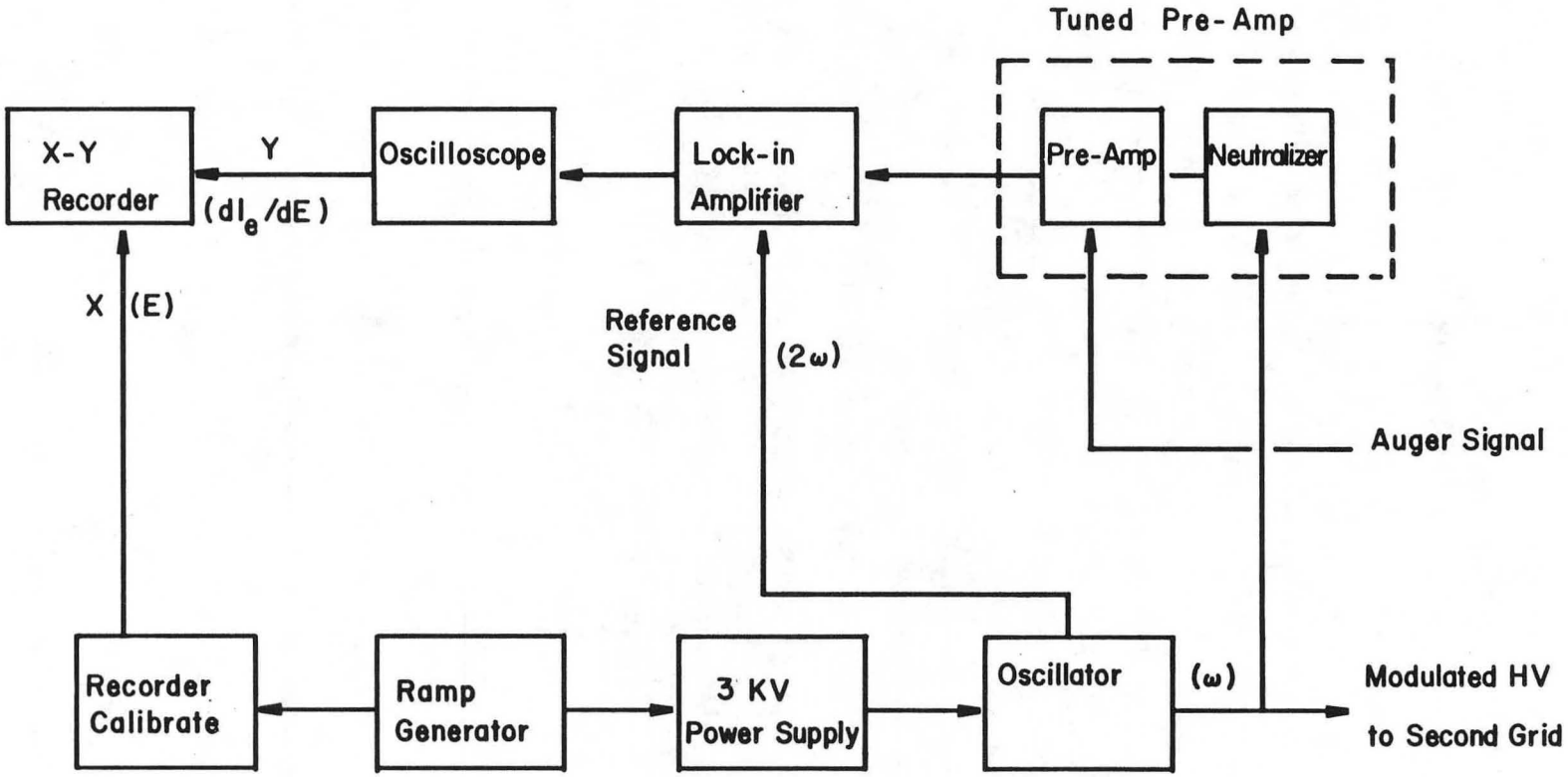

XBL 787-9662

Fig. 4. Block diagram of electronics used with the retarding field analyzer for Auger electron analysis.

above 100 eV. The modulation of the potential of the second grid results in the modulation of current collected by the phosphorus screen. The first harmonic of the modulation corresponded to the current of electrons with the same energy as the second grid. The phase-sensitive detector, set for the second harmonic of the 1000-Hz signal, produced an output signal corresponding to the derivative of the current of electrons with an energy equal to the potential of the second grid (dN(e)/dE). A 1.0 sec time constant was used for the phase-sensitive detector output. Voltage ramp rates were 50 V/min for Auger electron energies below 100 eV, and 100 V/min for Auger electron energies above 100 eV. Figure 5 shows the relationship between the electron current collected on the grid and the first and second derivatives of that value with respect to electron energy. An X-Y recorder recorded the output from the phase-sensitive detector as a function of the potential of the RFA.

2.3. Ellipsometry

Optical properties of the film covered surfaces were measured with a spectral-scanning ellipsometer developed earlier in this laboratory [refs. 1,20,21]. The ellipsometer used a polarizer-compensator-sample-analyzer (PCSA) configuration of optical components (fig. 6). A brief description of the apparatus follows.

The light source is a 75 watt high-pressure xenon lamp. The wavelength is varied by rotating a continuously variable interference filter (CVF monochromator). The CVF monochromator provides the ellipsometer with a spectral range of 350 to 740 nm. The filter has a band width ranging from 6 nm at a wavelength of 400 nm to 17 nm at a

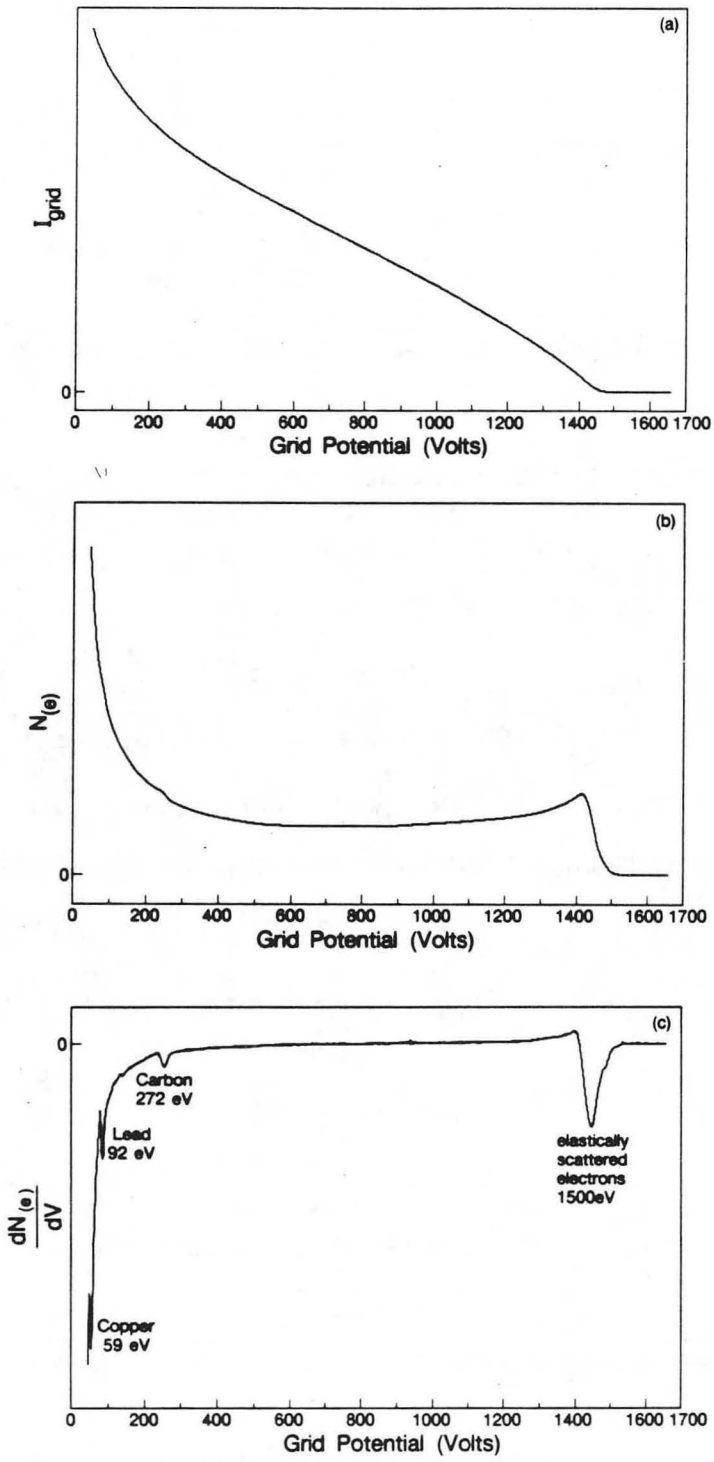

Fig. 5. Electron current energy distribution as collected by the retarding field analyzer: The sample consists of an island lead film upon a copper substrate. The retarding field voltage is ramped at 100 V/min from 30 to 1700 V. A 12 V peak-to-peak modulation of 1000 Hz is superimposed upon the retarding field. The excitation energy is 1500 eV. a) Electron current collected with energy above the retarding field potential (2nd grid potential), b) electron current (N(e)) of the specified energy (first derivative of fig. a), c) derivative of electron current of the specified energy (second derivative of Fig. a).

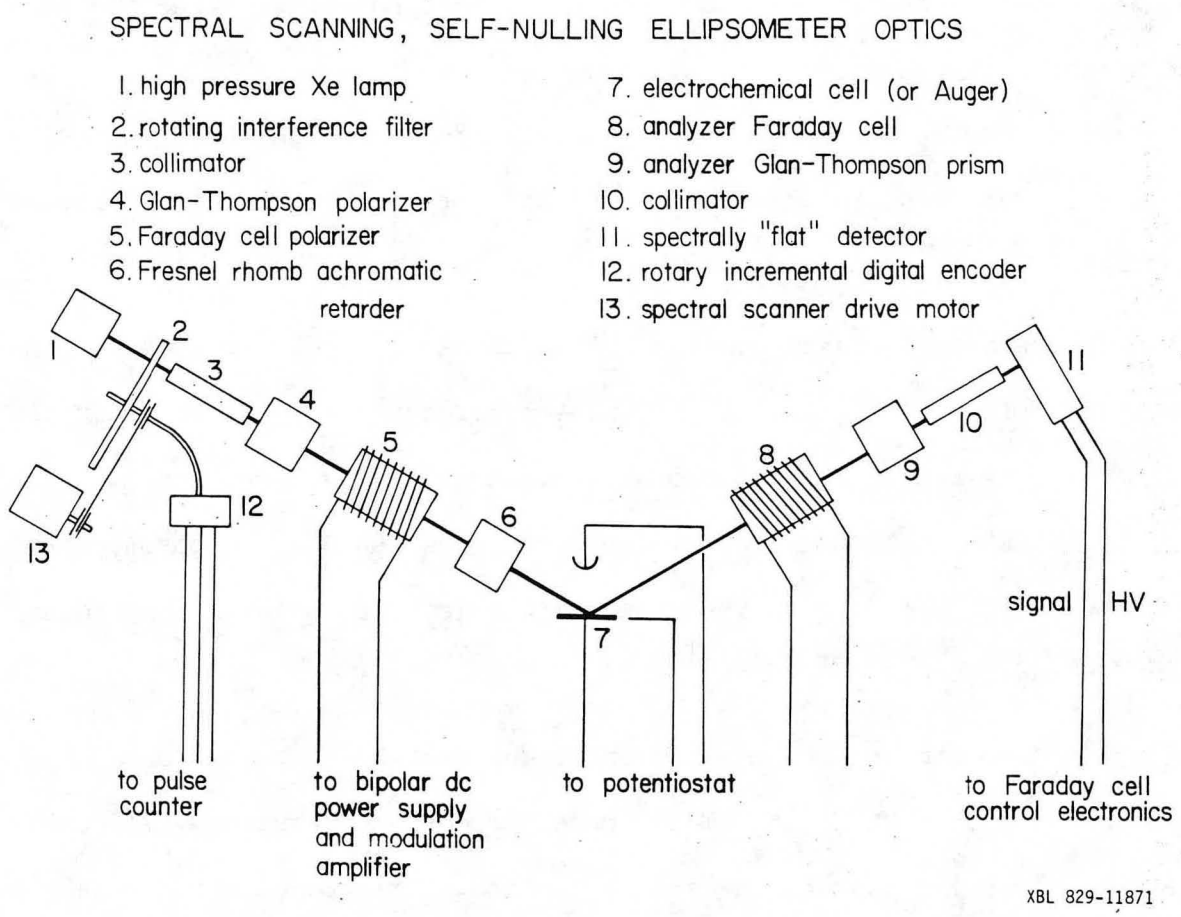

Fig. 6. Block diagram of the optical components of the spectroscopic ellipsometer with a polarizer-compensator-analyzer (PCA) configuration.

wavelength of 720 nm. A digital encoder is connected to the rotating filter to generate 400 pulses per revolution along with an initiatory pulse. The monochromator scans through its spectral range twice for each rotation. Data taken from the ellipsometer were thus recorded once with increasing and once with decreasing wavelengths for each run. The spectral scan rate was set at 30 nm/sec by the rotation speed of the filter. A complete rotation of the interference filter took 30 sec.

Monochromatic light from the CVF is linearly polarized by Glan-Thompsom prism. The azimuth of the transmitting axis of the polarized light is obtained by the addition of the magnetically induced rotation by the Faraday cell and the azimuth setting of the Glan-Thompsom prism. A Faraday cell and Glan-Thompsom-prism pair is used for both the polarizer and analyzer.

A Frenel rhomb performs achromatic quarter-wave retardation of the linearly polarized light. The Frenel rhomb compensator is located between the polarizer and the sample surface. The compensator uses a three reflection design to achieve wavelength independent retardation. The fast axis of the retarder is positioned at ±45 from the plane of incidence for all measurements.

The azimuths of the Glan-Thompsom prisms and the Frenel rhomb are set by the rotation of stepping motors attached to the individual components. The stepping motor can be controlled by commands from a computer interface. The stepping motors are geared such that each step results in a 0.02° change in the azimuth of the optical component.

The polarizer and analyzer Faraday cell currents are measured when the reflected light is extinguished (nulled). A feedback system using

the photomultiplier output controls the Faraday cell currents [ref. 21]. The Faraday cells are used to apply modulations to the azimuths of the polarizer and analyzer with a frequency of 10 kHz. The modulations of the polarizer and analyzer are separated by a 90° phase difference. The corresponding modulation of the photomultiplier output is used as an error signal for control of the Faraday cell currents. A phase sensitive detector separates the error signal from each Faraday cell.

A DIGITAL LSI-11 minicomputer was used to collect data during the spectral scans. Four-zone spectral scans were recorded with use of the data collection program "4ZONE" (Appendix C). The program 4ZONE performs three operations:

(1) Location of the Glan-Thompsom analyzer and polarizer azimuths for a null at a -45° azimuth of the compensator.

(2) Repositioning of the analyzer, polarizer, and compensator azimuths for the other three zones.

(3) Data collection of the analyzer and polarizer Faraday cell currents.

A null is found manually by minimizing the photomultiplier current and then minimizing the Faraday cell current through adjustments of the azimuths of the Glan-Thompsom prism for the analyzer and polarizer. After locating the null, the program initiates a spectral scan. After completing the spectral scan, the azimuths of the polarizer, compensator, and analyzer are repositioned with the stepping motors to scan in another zone.

The program records the polarizer, compensator, and analyzer positions for each zone. Data for each zone are collected in separate files for later conversion to delta and psi values. The measured delta and psi values from each zone were averaged following the completion of the four-zone measurements.

3. Optical Model

A two-film optical model was used to interpret the measured optical properties of the ion bombarded films. Both of the films were allowed to vary in porosity. The effect of porosity on the optical properties of a porous medium were interpreted with an effective medium model. The outermost film was allowed to be of a pitted or island structure (fig. 7). A coherent superposition model was used to interpret optical properties of pitted or island films. Two basic combinations of films were used (fig. 8); (1) an lead oxide film with an underlying lead film and (2) a pitted lead film upon an underlying lead film. In each case the ambient medium was vacuum and the underlying substrate was copper.

The optical properties of the continuous film can be described by an isotropic and homogeneous film model [ref. 22]. If the refractive index of the film medium is known only the thickness is needed to describe film.

Three effective-medium models are available to model the optical properties of a porous medium:

(1) Lorentz-Lorenz [refs. 24,25,26]

(2) Maxwell-Garnett [refs. 23,24,25]

(3) Bruggeman [refs. 23,24,25]

This investigation used the Bruggeman effective-medium approximation for the apparent refractive index of the film medium.

The Bruggeman equation is a special case of a general rule for mixing the dielectric properties of a multicomponent medium.

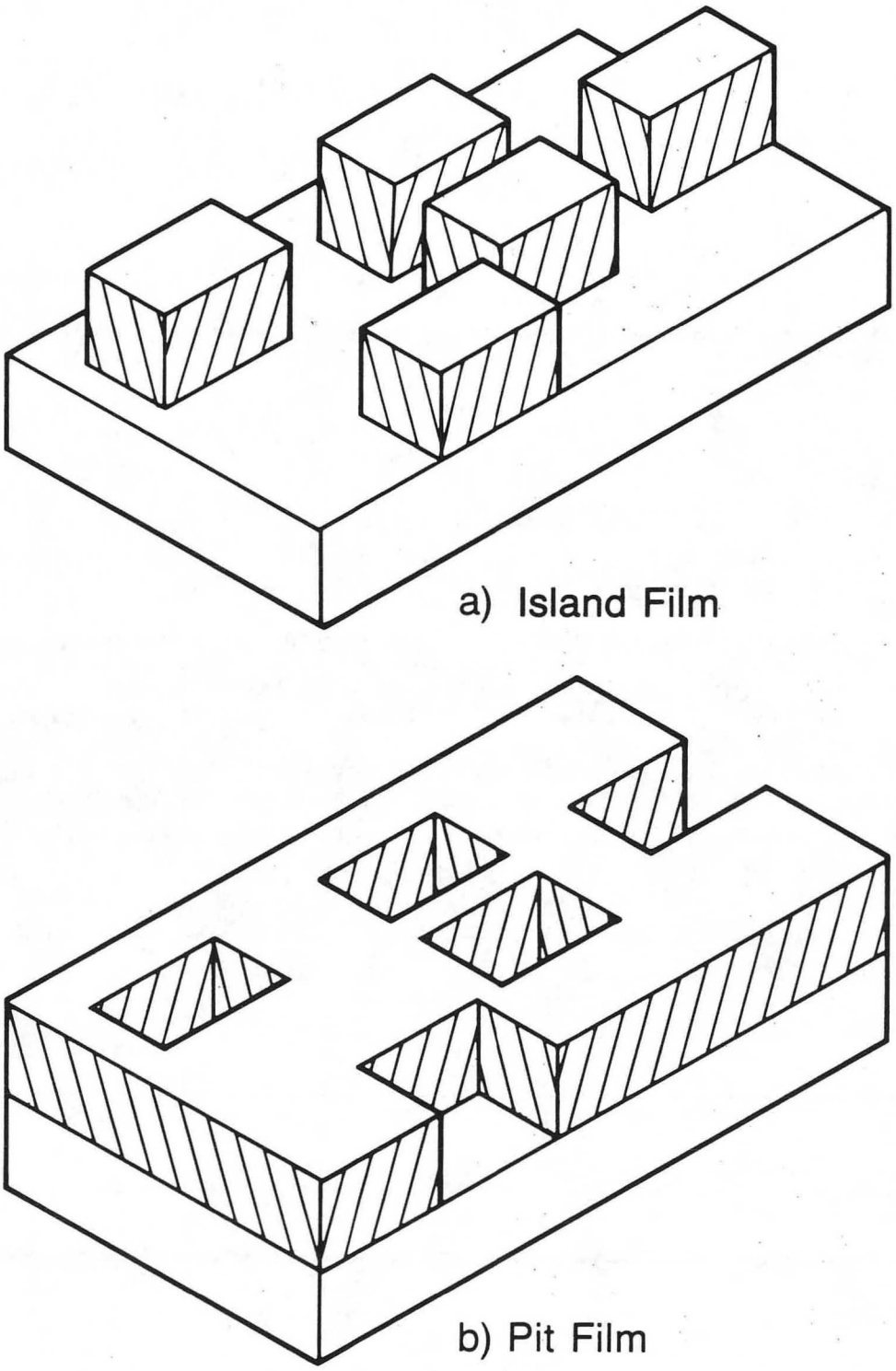

XBL 847-10702

Fig. 7. Diagram of island and pitted films. a) Island film, continuous substrate surface, b) pitted film, continuous film covered surface.

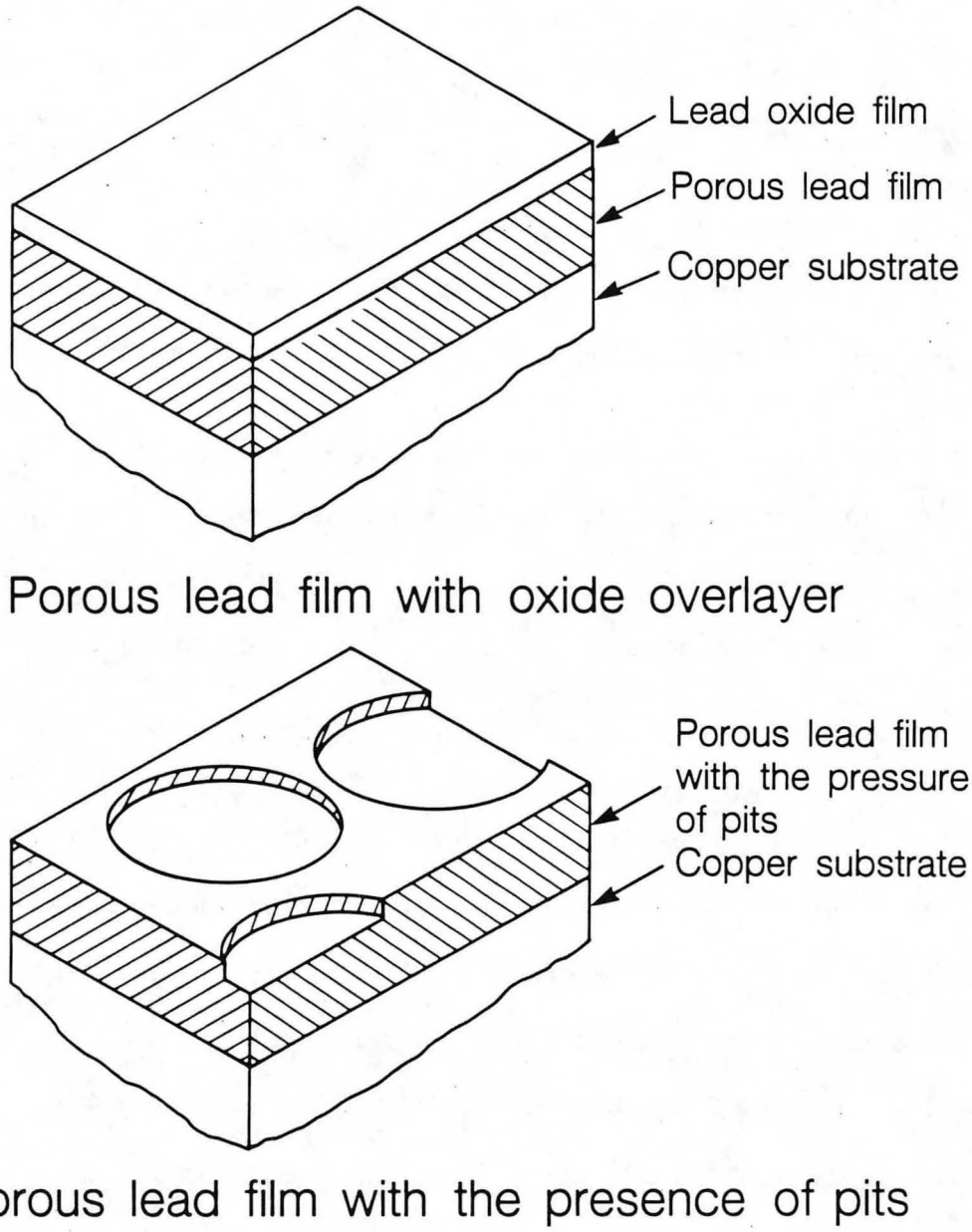

Fig. 8. Schematic of model surfaces used for interpreting spectroscopic ellipsometry measurements.

$$\frac{\hat{\varepsilon} - \hat{\varepsilon}_h}{\hat{\varepsilon} + 2\hat{\varepsilon}_h} = \sum_{i=1}^{n} \frac{\hat{\varepsilon}_i - \hat{\varepsilon}_h}{\hat{\varepsilon} + 2\hat{\varepsilon}_h}$$

where

$\hat{\varepsilon}$ is the complex dielectric function of the effective medium,

$\hat{\varepsilon}_h$ is the complex dielectric function of the host medium, and

$\hat{\varepsilon}_i$ is the complex dielectric function of the ith component.

A porous film of a single material with known refractive indices has two terms in the summation. The two terms represent the weighted contribution of the polarizing abilities of film material and the pore material. The dielectric function is related to the refractive index by the function,

$$\hat{n} = \hat{\varepsilon}^{1/2}$$

where n is the complex refractive index. The dielectric constant of the host medium in the Bruggeman equation is set equal to the effective medium dielectric constant. The Bruggeman effective medium equations are self-consistent over the complete range of volume fractions.

The island and pitted films optically behave the same. The optical properties are a function of the relative portions of bare and film-covered surface. The optical properties are not a function of whether the bare surface or film-covered surface is continuous. The films are defined as being islands or pits depending on whether the film-covered or bare surface is continuous (fig. 7).

The island film is modeled with the coherent superposition model [refs. 1,2]. Overall reflection coefficients for the island covered sur-

face are calculated from the reflection coefficients of the bare and film-covered surfaces. The reflection coefficients of the bare and film-covered surfaces are weighted according to the fraction of surface covered by each.

$$r_\nu = \theta_f \, r_{\nu,f} + (1 - \theta_f) \, r_{\nu,s}$$

The overall reflection coefficients represent a coherent super-position of polarization states from reflection on adjacent bare and film-covered surface elements.

The dimensions of the islands parallel to the surface must be smaller than the transverse and longitudinal coherence length of the ellipsometer light source: Otherwise the light would be incoherently superimposed [ref. 27]. The light source used in this study had a longitudinal coherence length of 16 μm and a transverse coherence length of 10 μm at 400 nm [ref. 1].

For multilayer calculations the apparent optical constants were calculated for the layer next to the substrate and then were used as substrate optical constants for the next layer.

The parameters of the models were optimized to fit the observed optical properties with calculated optical properties. A univariate search routine for the minimum sum-of-squares error between the calculated and measured values of delta and psi was used. The program WLGOGO was developed for this purpose by J.C. Farmer [refs. 1,28]. Measured values of delta and psi for every 25 nm between 450 and 650 nm were used in the optimization. The Δ-ψ pairs could be considered a separate measurement. The univariate search routine operated by varying each parame-

ter a fixed increment in the direction which minimizes the error. The sum-of-squares error, S, is defined by

$$S = \sum_{i=1}^{n} [(\Delta_{C,i} - \Delta_{M,i})^2 + (\Psi_{C,i} - \Psi_{M,i})^2]^{1/2}$$

where N is the total number of Δ-ψ pairs at the same wavelength, subscript c is the value calculated by the model, and subscript m is the measured value. A model variance, σ^2, can be approximated by

$$\sigma^2 = S_{MIN}/df = S_{MIN}/(2N - P)$$

where S_{min} is the sum-of-squares error at the best fit of model parameters and P is the total number of adjustable parameters. The parameter variance SE(p), is defined by

$$SE(p) = \frac{\sigma^2}{\frac{1}{2}\frac{\partial^s S}{\partial p^2}}$$

where p is the parameter value. The denominator in the above equation was approximated by

$$\frac{1}{2}\frac{\partial^2 S}{\partial p^2} \simeq \frac{S_{(+)} + S_{(-)} - 2S_{MIN}}{2(\Delta p)^2}$$

where delta p is the parameter search increment, S(+) is the value of S with a positive increment of the value of p from its optimum value, and S(-) is the value of S with a negative increment of the value of p from its optimum value.

4. Results and Discussion

4.1. Refractive Index of Copper and Lead

The spectral dependence of the refractive index was measured with ellipsometry for both copper and lead. The measured refractive indices were then used as parameters for numerical modeling of the optical properties of lead films following ion bombardment.

The refractive indicies were calculated based on the assumption that the interface between the metal and vacuum was optically smooth and that the metal was isotropic. There were no corrections for the microroughness of the surface that may have been present due to the preparation of the surface. Ion bombardment damage has been modeled in literature as a porous film [refs. 16,17].

A copper surface was prepared by mechanical polishing with 0.05 μm alumina. The surface was ion bombarded with 1100 eV argon ions for 60 min. to remove copper oxide and any contaminants. The optical properties were measured within the ultrahigh vacuum chamber. Figure 9 shows the measured refractive indices and some reported values from literature [ref. 29].

The optical properties of the copper surface became stable with respect to ion bombardment duration following removal of the oxide layer. In addition the optical properties were reproducible between different copper samples. Figure 10 shows the spectral dependence of delta and psi for four separate copper samples after extended ion bombardment.

A lead surface was prepared by the evaporation of 99.999% lead wire onto a polished copper substrate in ultrahigh vacuum. The film was

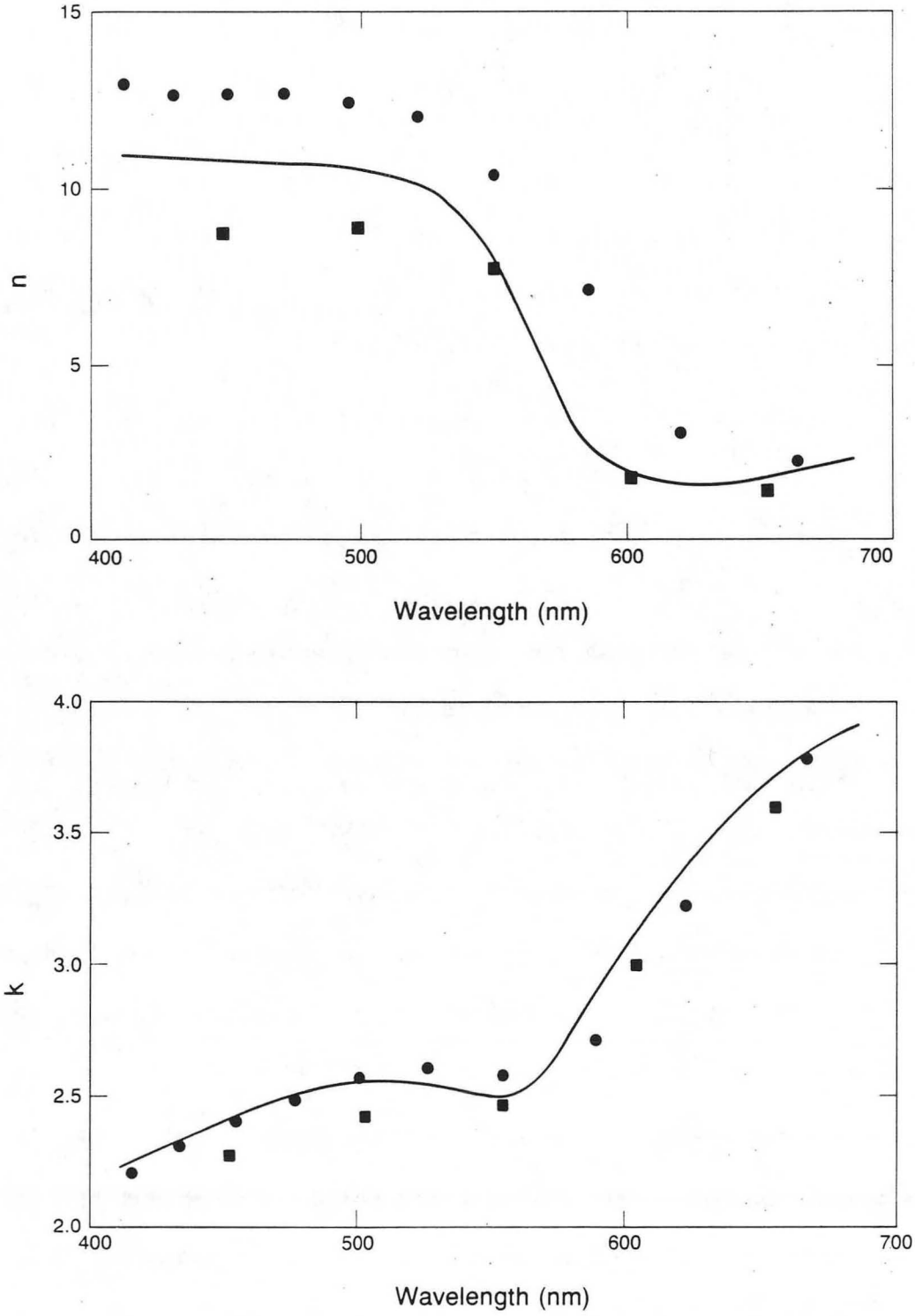

XBL 844-10454A

Fig. 9. Spectral dependence of the refractive index of bulk copper following 60 min of 1100 eV Ar ion bombardment at a 75 angle of incidence. Literature values for clean surface [Refs. 29,30]. a) refractive index, b) extinction coefficient.

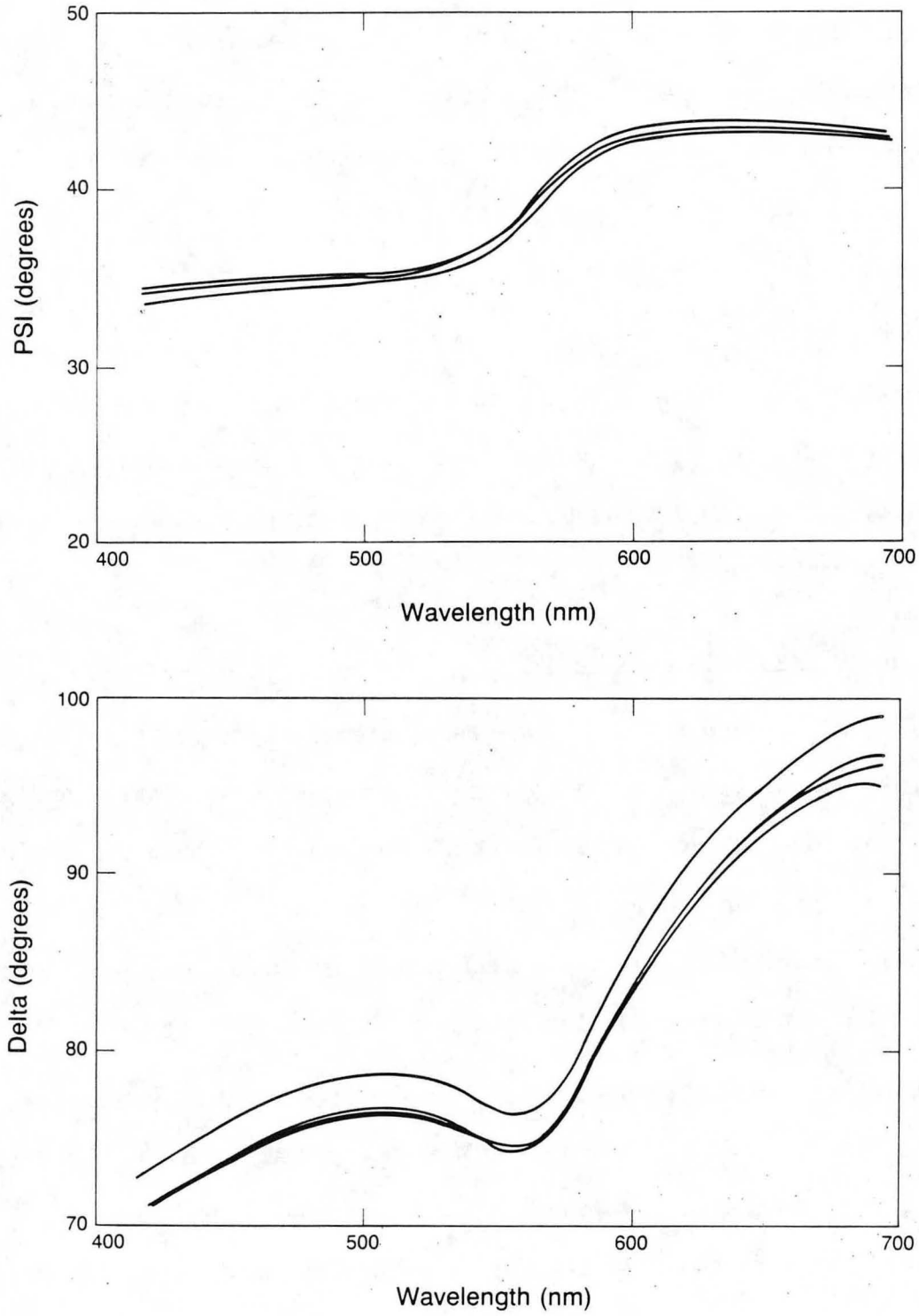

XBL 844-10456A

Fig. 10. Spectral ellipsometric measurements from four separate copper samples following ion bombardment with 1100 eV Ar ions. The measurements were taken at sputter times greater than that required to reach steady optical properties of the surface. a) delta, b) psi.

optically opaque such that the copper substrate did not affect the measured optical properties. A 10 min session of ion bombardment was used to clean any oxide or contaminants from the surface. The measured refractive index and some reported literature values [ref. 36] are shown in fig. 11.

Auger electron spectroscopy of both the lead and copper surfaces indicated the presence of oxygen and carbon. Ion bombardment eliminated the oxygen Auger peak; the carbon Auger peak remained but at a reduced intensity. A weak sulfur Auger peak from the copper surface was detected after ion bombardment.

4.2. Pit Formation in Lead Films

The optical properties of an electrochemically deposited lead film of 0.039 C/cm^2 (369 Å compact) were measured intermittently throughout 125 min of ion bombardment with 1100 eV Ar ions. The optical properties, delta and psi are shown in fig. 12. The optimization routine "WLGOGO" was used to obtain information of the structure of the surface from the ellipsometric measurements (Tables 2 and 3).

Initially and after 5 min of ion bombardment the surface was modeled as a lead substrate of 20% porosity with an overlying uniform oxide layer. The refractive index of the oxide was taken to be 2.5-0.0i, which was approximated from literature values of PbO minerals [ref. 30]. The oxide thickness was determined to be 31 A at the beginning of the film profiling session.

Table 2. Optical model parameters for the ion bombardment C/cm^2 of a electrochemically deposited lead sample of 0.039 (369 Å compact). The deposit was made in the pressence of Rhodamine-b chloride in a sodium perchorate supporting electrolyte. The Optical model parameters are tabulated as a function of ion bombardment duration of 1100 eV Ar ions. The optical model consists of either an lead-oxide or porous-lead- island film upon a porous lead film with a copper substrate.

Film Model Parameters					
Time	Porosity (%)	Island Coverage (Å)	Island Height (Å)	Compact Film Height (Å)	Oxide Film Height
0	20.	NA	NA	OP	31
5	20.	NA	NA	OP	11
15	18.	0.82	OP	110	0
25	16.	0.78	OP	77	0
35	19.	0.74	OP	30	0
45	19.	0.68	OP	0	0
55	20.	0.50	OP	0	0
65	20.	0.30	OP	0	0
75	18.	0.14	OP	0	0
85	19.	0.08	OP	0	0
95	16.	0.04	OP	0	0
105	23.	0.02	OP	0	0
115	00.	0.01	360	0	0
125	NA	0.00	0	0	0

OP -- Opaque, the model is insensitive to height since the light is attinuated by the film.

NA -- Not Applicable

Table 3. Fraction of copper substrate covered with lead as a function of ion bombardment duration of 1100 eV Ar ions for a electrochemically deposited lead sample of 0.039 C/cm/cm (369 Å compact). The surface coverage was determined from optical modeling of the optical properties and from Auger electron spectroscopy.

	Fraction of Surface Covered by Lead	
Time	AES	Ellipsometry (Island Model)
0	1.00	1.00
5	1.00	1.00
15	1.00	1.00
25	0.98	1.00
35	1.00	1.00
45	0.76	0.68
55	0.57	0.50
65	0.44	0.30
75	0.24	0.14
85	0.16	0.08
95	0.16	0.04
105	0.08	0.02
115	0.02	0.01
125	0.01	0.00

After 15, 25, and 35 min of sputtering the measured optical properties of the surface were modeled with a pitted porous film. The porosity of the film was determined to be 20%. A comparison of the measured delta and psi parameters with those calculated by the pitted porous film model of the surface is shown in fig. 13. The measured values in fig. 13 corresponed to 35 min of ion bombardment. The fact that the pit depth on the real surface follows some distribution about the average pit depth may account for the discrepancy between the calculated and measured spectra.

Following 45 min of ion bombardment the copper substrate became exposed as was indicated by AES and ellipsometric measurements (Table

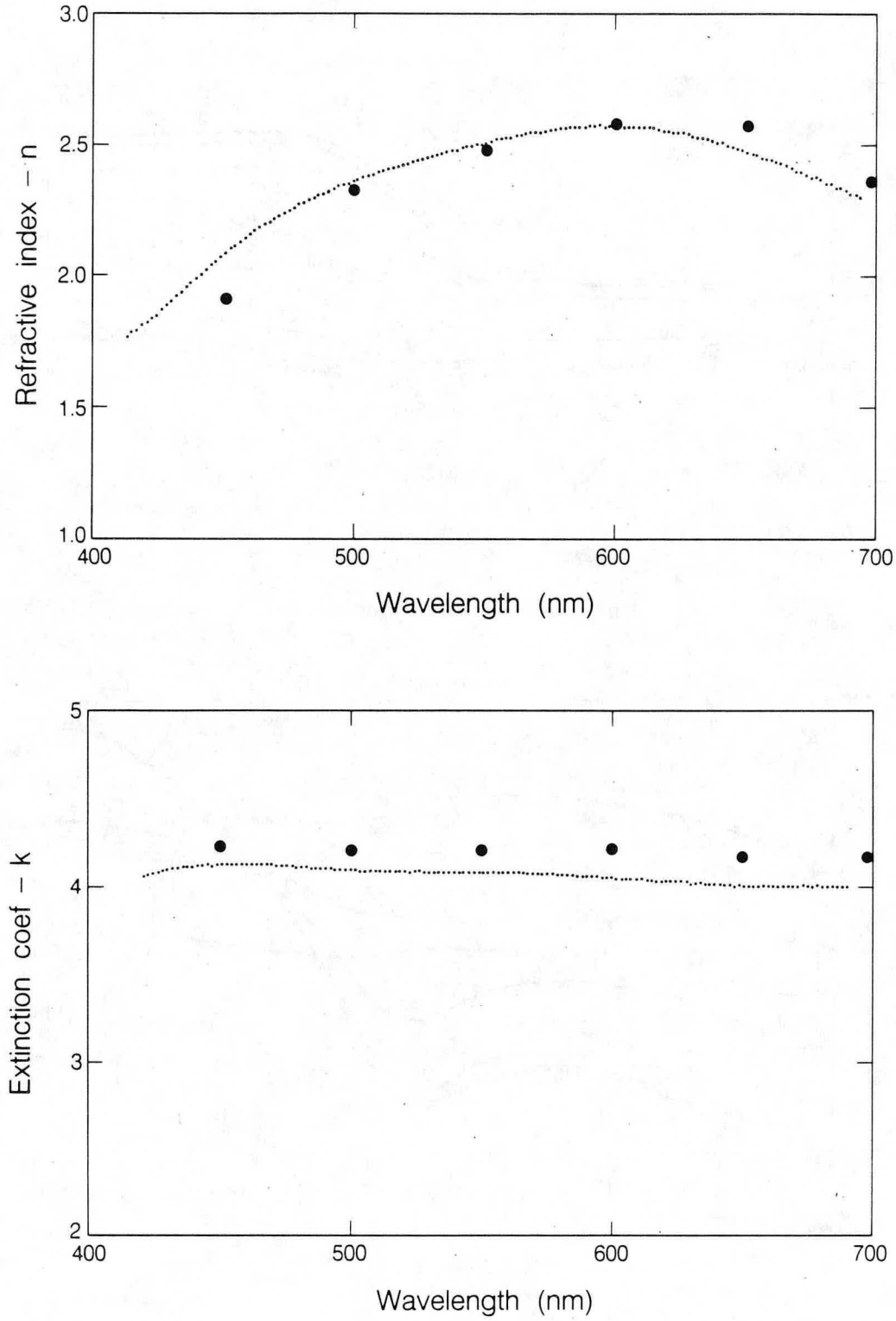

Fig. 11. Spectral dependence of the refractive index of vapor deposited lead following 10 min. of 1100 eV Ar ion bombardment. The ion beam intersected the surface at an angle of incidence of 75. Literature values (•) are shown for comparison from Lijenvall, Mathewson, and Myers [Ref. 36]. a) Refractive index, b) Extinction coefficient.

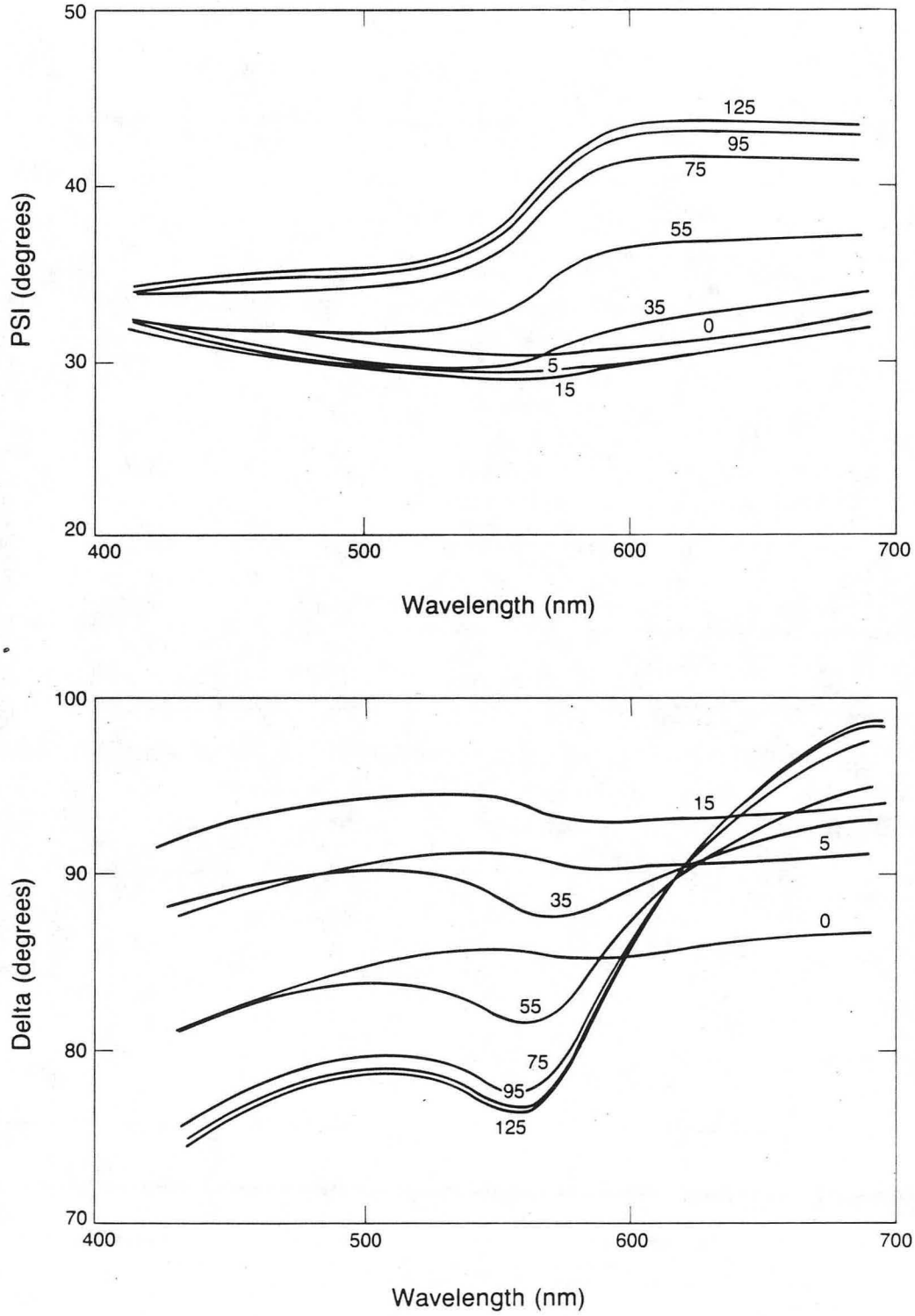

XBL 844-10453A

Fig. 12. Spectral ellipsometric measurements from a electrochemical lead deposit from 0.039 C/cm^2 (340 Å) intermittently through out 125 min of 1100 eV Ar ion bombardment. The changes in the optical properties reflect the removal of oxide for the first 15 min and the generation of pits throughout the 125 min of sputtering. The spectral scan after 125 min of ion bombardment is that of bare copper. The angle of incidence of the ion beam is 75°. a) delta, b) psi.

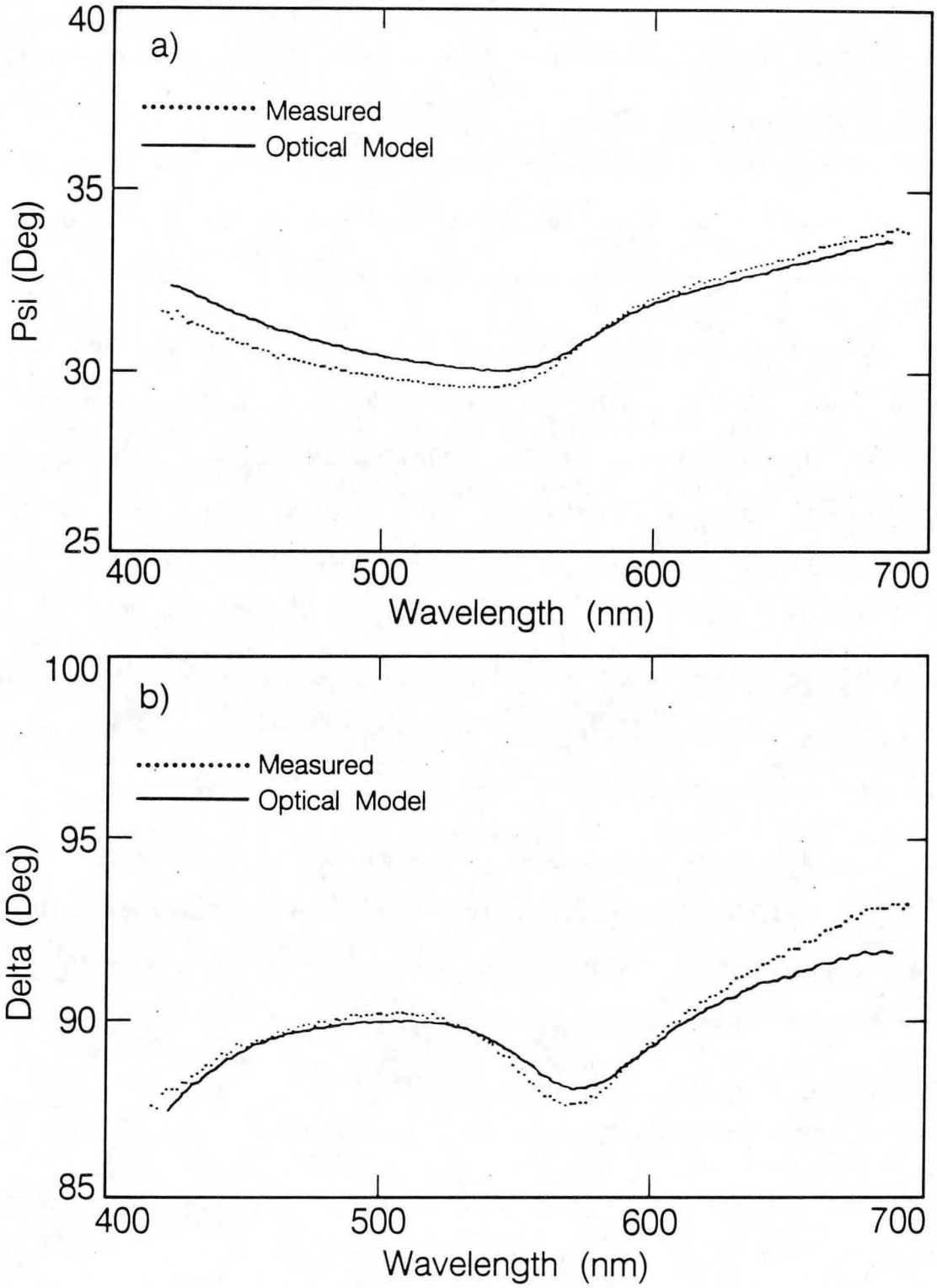

XBL 848-8659

Fig. 13. Comparison of the measured delta and psi to the calculated values for the 0.039 C/cm^2 (369 Å compact) lead deposit following 35 min. of ion bombardment. The optical model consists of a 0.74 coverage of lead islands with an underlying 30 Å lead film. Both the islands and continuous film have a porosity of 0.2. The substrate is bulk copper. a) delta, b) psi.

2). The ellipsometric and AES mesurements indicate the increasing coverage of pits with ion bombardment time between 45 and 125 min. Figure 14 is a comparison of the lead coverage of copper as calculated from ellipsometric and AES measurements. Following 125 min of ion bombardment, ellipsometric measurements indicate a bare copper surface and Auger spectroscopic measurements indicate a 1% coverage of lead.

Scanning electron microscopy was performed on the surface of an electrochemically deposited Pb film of 0.078 C/cm^2 following ion bombardment with 1100 eV Ar ions. The initial thickness was calculated to be 780 Å using the bulk density of lead. The film was bombarded for 85 min before Cu was detected with AES. Oxygen was indicated in the AES of the surface before ion bombardment. Figure 15 is a scanning electron micrograph of the surface which shows the presence of 1 μm diameter pits. There is no apparent orientation of the pits with the ion beam orientation on the surface.

In an effort to determine whether electrolytic deposition of the lead was responsible for island formation under ion bombardment, vapor deposits made in a VARIAN evaporator were investigated. Figure 16 is a scanning electron micrograph of a vapor deposit on copper electrode polished with 1 μm diamond paste. There were no pits present in the film prior to ion bombardment.

A vapor deposit on a copper substrate polished with 0.05 μm diamond paste was subjected to ion bombardment and subsequently investigated with AES and spectroscopic ellipsometry. The lead deposit was optically opaque to the copper surface. The optical properties of the film before ion bombardment indicated an oxide layer of 35 Å. Auger electron

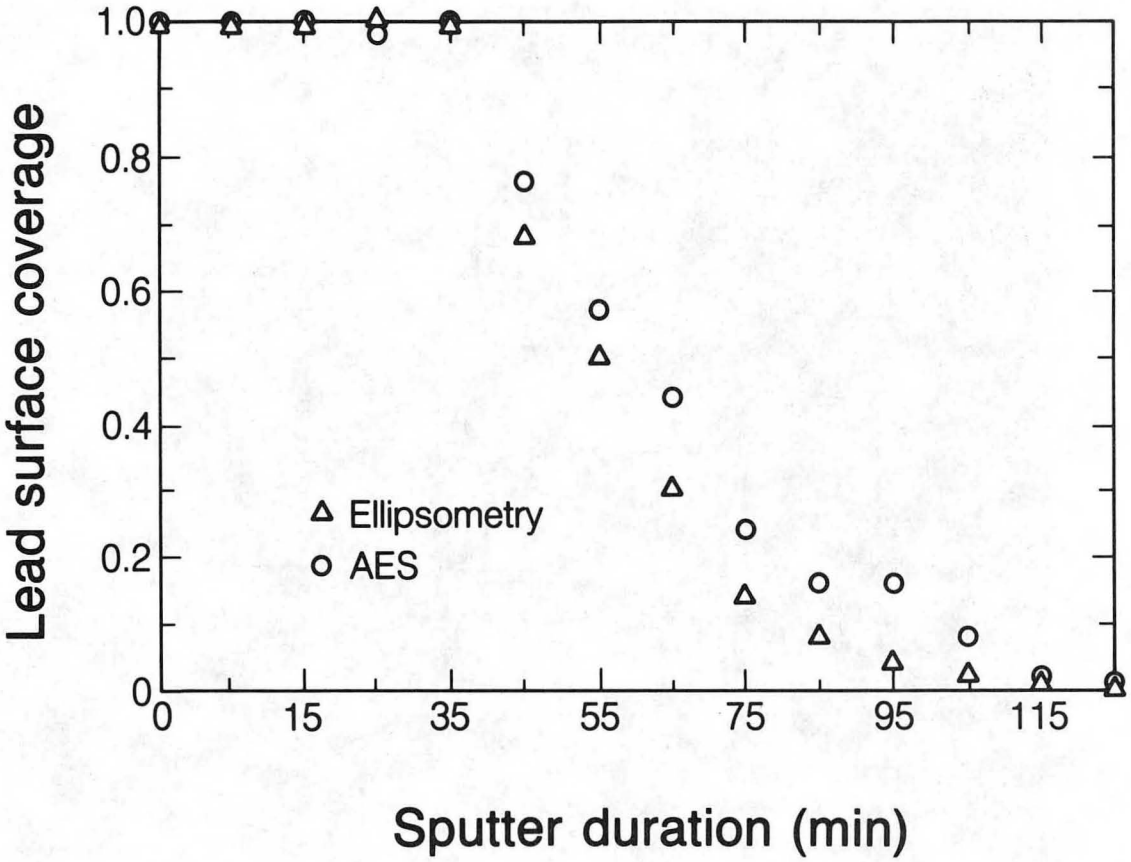

XBL 847-9848

Fig. 14. Fraction of the copper surface covered by lead as a function of sputter duration for a 0.039 C/cm^2 (369 Å compact) electrochemical deposit of lead. The coverage is determined with Auger electron spectroscopy and spectroscopic ellipsometry. The ion source consisted of 1100 eV ar ions with an angle of incidence on the sample surface of 75°.

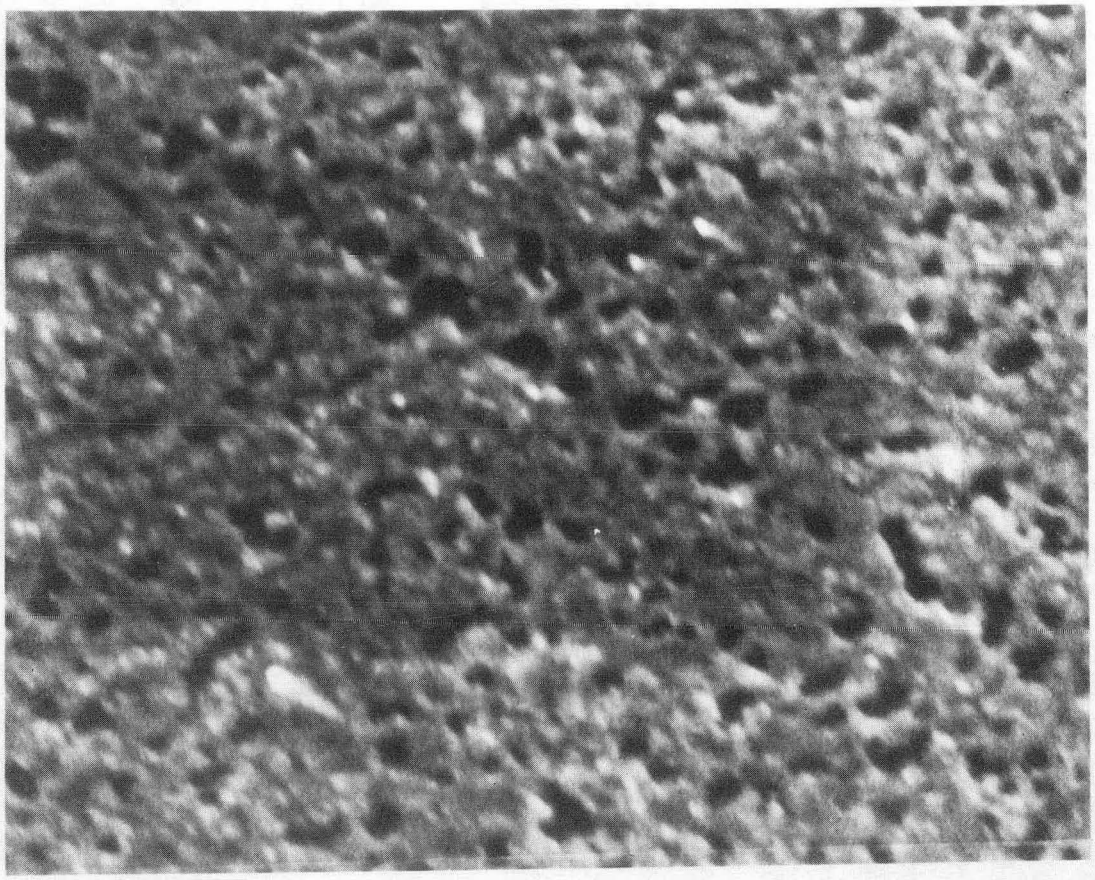

2.0μm XBB 844-2541

Fig. 15. Scanning electron micrograph of a electrochemical lead deposit of 0.079 C/cm^2 (738 Å compact) following 65 min of 1.1 keV Ar ion bombardment at an angle of incidence of 75°. The micrograph shows severe pitting of the lead film. The pits are on the order of 1 μm across and penetrate into the underlying copper substrate.

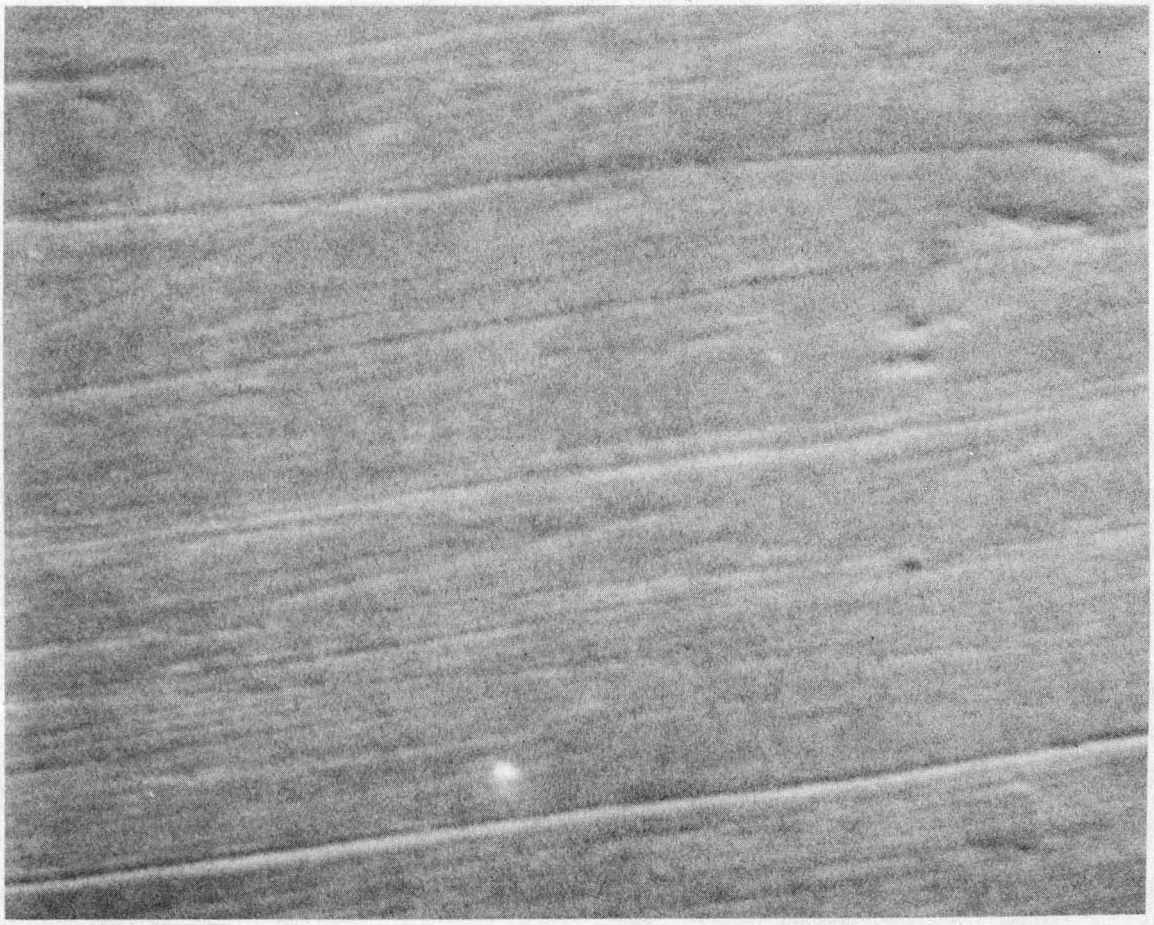

2.0μm XBB 844-3116

Fig. 16. Scanning electron micrograph of a Pb vapor deposit made with a VARIAN evaporator under a background pressure of 10^{-4} torr. A 1 μm polishing paste was used on the copper substrate rather than the 0.05 μm polish used on the substrate of the ion bombarded deposits. No pits are present.

spectroscopy also indicated the presence of oxygen before ion bombardment. Ion bombardment was performed with 1100 eV Ar ions. The vapor deposit was ion bombarded for 45 min at which point AES indicated a 67% coverage of Pb. Interpretation of the optical properties by the island film model indicated a 66% coverage of lead. In addition an increase in light scattering from the surface was noticed.

Without further ion bombardment the sample was removed for scanning electron microscopy. In transfer to the microscope the sample was exposed to air. Figure 17 is a scanning electron micrograph of the vapor deposit following the 45 min of ion bombardment. The presence of pits 1 μm in diameter can be seen. There is no apparent orientation of the pits with respect to the direction of ion bombardment.

To determine the effect of a lead oxide film present in the above lead deposits, two vacuum vapor deposits were made within the AES and ellipsometry equipped UHV chamber. A transfer of the sample involving an exposure to oxygen was thus avoided. Morphological changes which were induced by ion bombardment were similar to that observed on previous films. Figures 18 and 19 show scanning electron micrographs of the surfaces of a 100 Å and an opaque (>300 Å) vapor deposit respectively. The thickness of the films were determined from ellipsometric measurements. The width of pits formed in the 100 A deposit was on the order of 0.2 μm compared to the 1.0 μm observed on the thicker deposits.

The possibilty of pit formation due to the presence of carbon was investigated. The carbon species is more difficult to sputter from the surface than lead (Table 1); thus patches of lead covered by carbon may be protected from the bombarding ions. Should the carbon be protecting

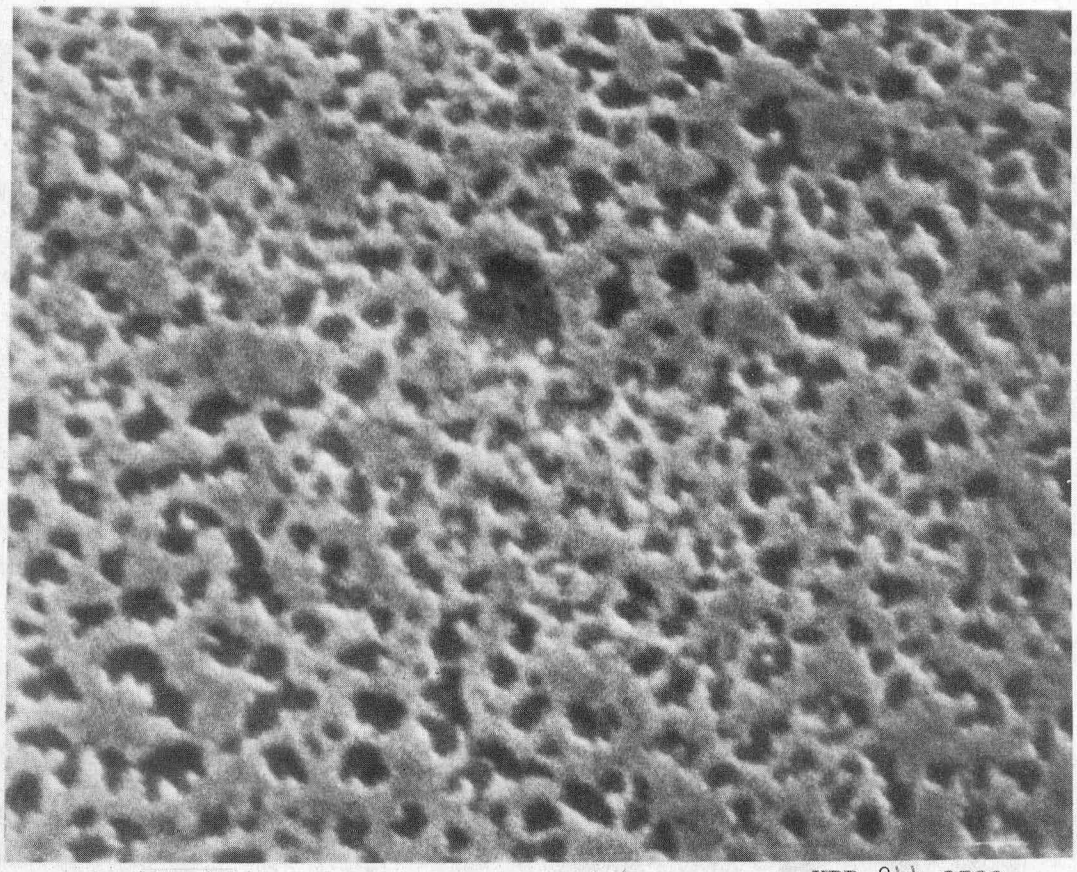

2.0μm

XBB 844-2539

Fig. 17. Scanning electron micrograph of a Pb vapor deposit after 45 min of 1 keV Ar ion bombardment. Spectroscopic ellipsometry measurements fitted with a coherent superposition model of the pits indicates a 68% coverage of the copper surface by lead of 20% porosity with a thickness greater than 450 Å. The photo shows severe pitting similar to that in fig. 15.

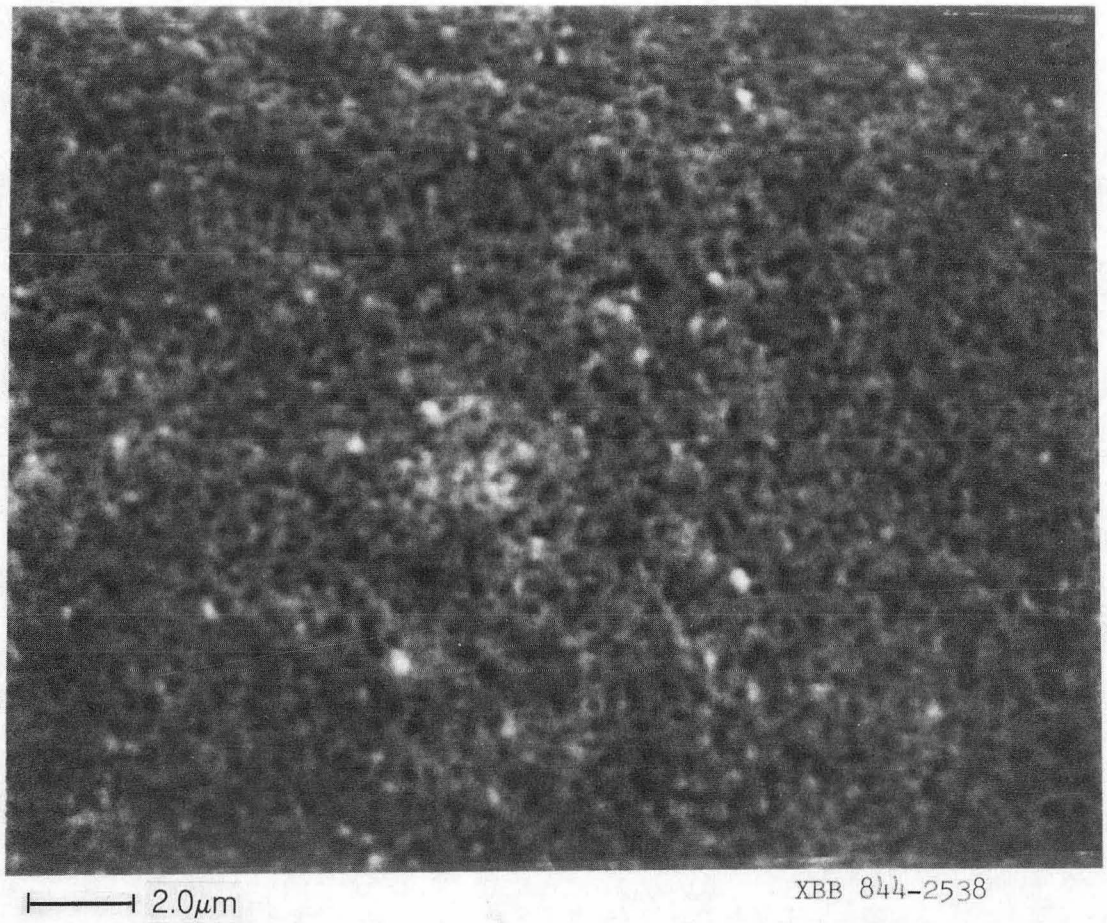

Fig. 18. Scanning electron micrograph of a vapor deposit of lead formed in the ultrahigh vacuum chamber with a background pressure of 10^{-7} torr following 10 min of 1.1 keV Ar ion bombardment. Interpretation of the optical measurements with a compact film model indicated an initial thickness of 100 Å before ion bombardment. No oxide was indicated. Pitting similar to that of figs. 15 and 17 is present with pit diameters of about 1000 Å.

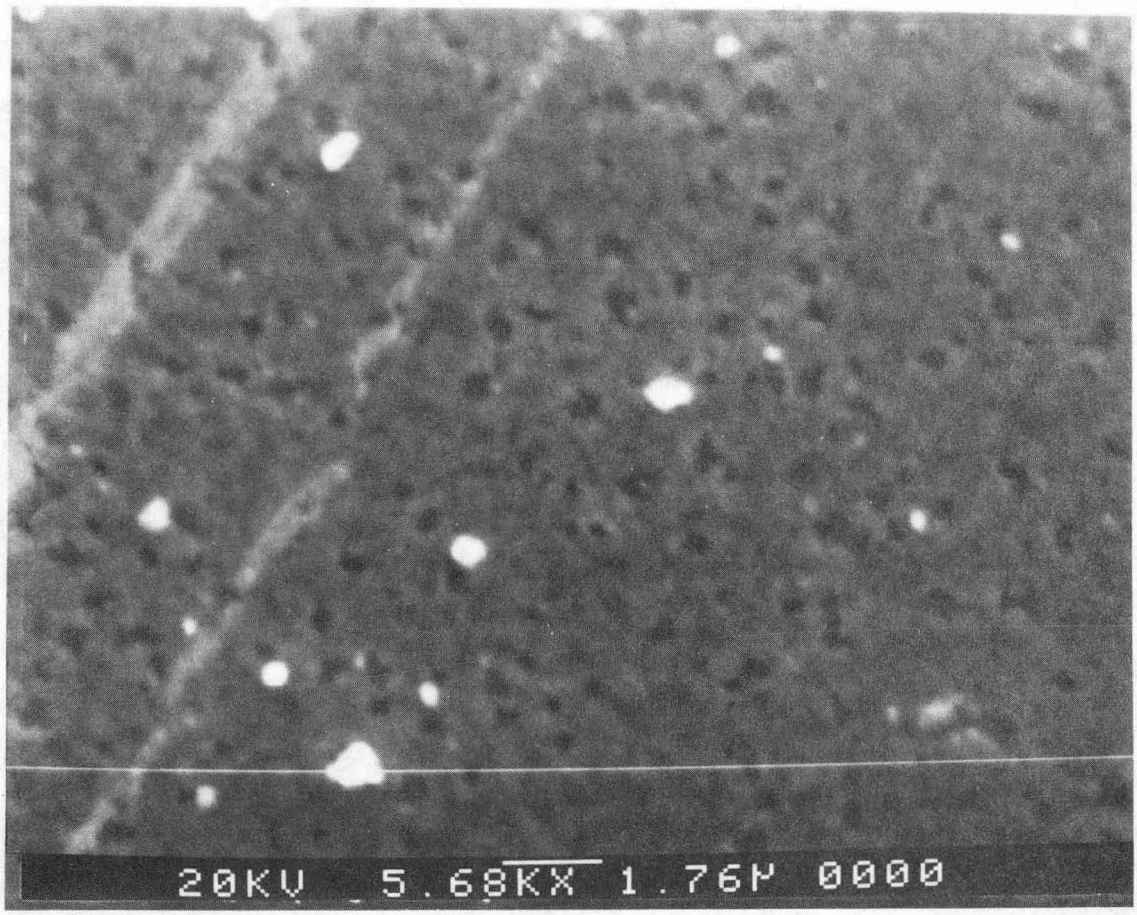

XBB 844-2537

Fig. 19. Scanning electron micrograph of a vapor deposit of lead formed in the ultrahigh vacuum chamber with a background pressure of 10^{-7} torr following 65 min of 1.1 keV Ar ion bombardment. The film was thicker than 300 Å and did not have an oxide layer before ion bombardment. Pitting similar to that in Figs. 15 and 17 are shown.

the lead surface, it would be expected that the AES carbon peak height would vary proportionally with the lead surface coverage. A comparison of the carbon peak height to the island coverage is shown in fig. 20. After 45 min the island coverage began to decrease rapidly. Initially as the island coverage began to decrease, the carbon peak also decreased but after 55 min of ion bombardment the carbon peak began to increase with removal of the lead islands. The carbon peak reached a maximum of twice the initial height after 85 min of ion bombardment. Following the removal of the lead from the copper surface, the carbon peak returned to its initial height. The increased carbon peak height towards the end of the lead film removal may be attributed to rhodamine-b dye incorporated within the lead deposit or at the copper-lead interface.

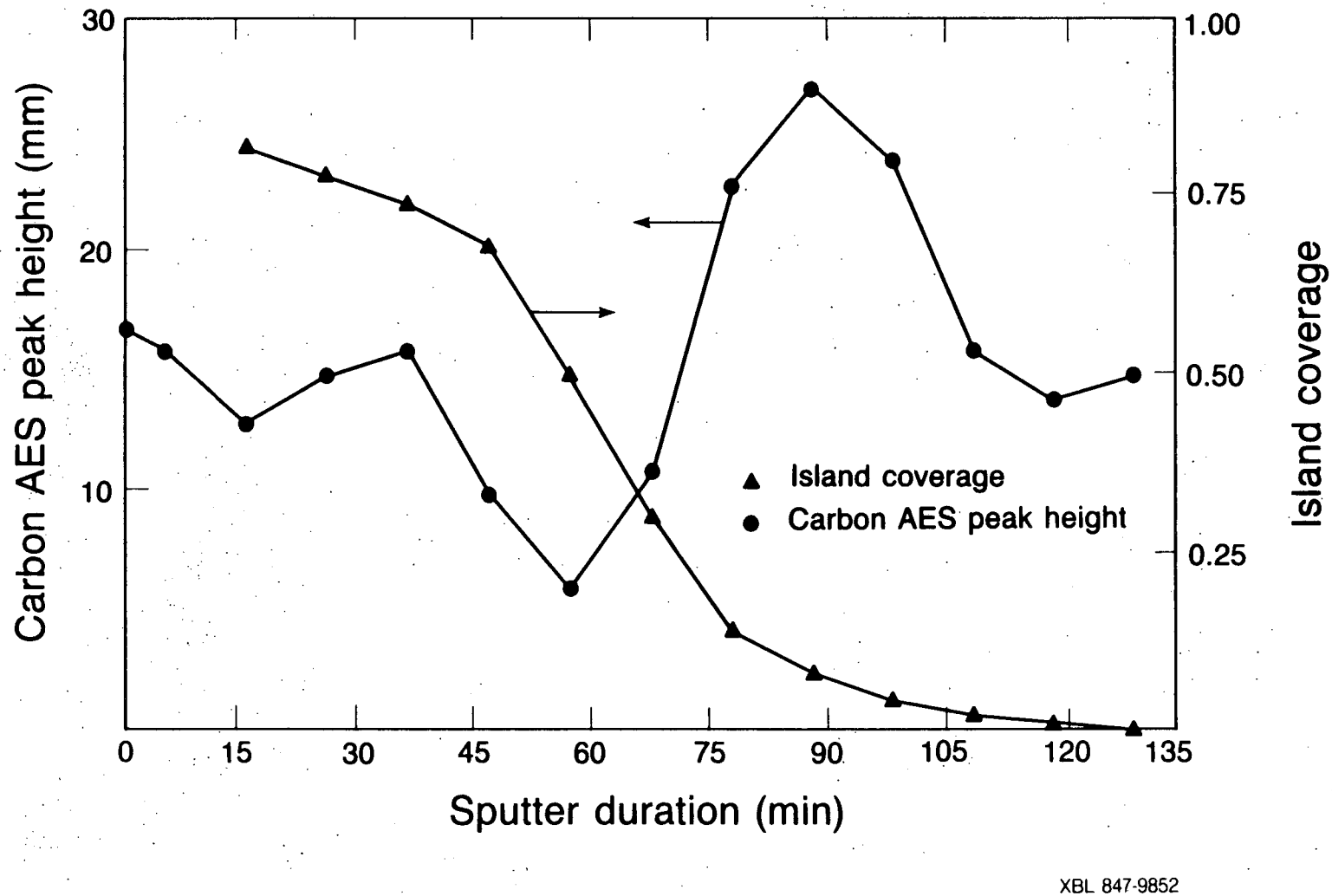

Fig. 20. Comparison of the island coverage with the carbon AES peak height as a function of the ion bombardment duration for the 0.039 C/cm^2 (369 Å compact) lead deposit.

5. Conclusion

Thin uniform lead films on copper are not uniformly removed by ion bombardment. The films become pitted following bombardment by low-energy 1100-eV argon ions. Pit formation does not seem to depend on the presence of an oxide layer, rather it appears to be a result of the sputtering process. No lead deposits on substrates other than copper were investigated, so no comparison is available to ascertain whether there is a substrate effect. The results of this study demonstrate the problems associated with using ion bombardment to obtain composition profiles of thin films.

The measured optical properties of the ion bombarded lead films are best explained by an island-film model. The island film model is based on the coherent superposition of the polarization states of reflected light from bare and film covered surface. The agreement of predictions of the optical model with the observed spectroscopic measurements confirms the appropriateness of using coherent super-position to model island-film surfaces.

Acknowledgments

The author wishes to thank Dr. Rolf H. Muller for his helpful suggestions during the preparation of this dissertation. This work was done with support from the Department of Energy under contract No. DE-AC03-76SF00098.

6. APPENDIX A. Auger Electron Spectroscopy

Auger electron spectroscopy (AES) is a surface analysis technique for determining the composition of a surface. Due to the short escape depth of the Auger electron emissions, AES has a depth resolution of 20 to 30 Å. Figure 21 shows the universal escape depth curve for electrons [ref. 31]. Auger electron emissions are stimulated by either electron or X-ray sources of 1 to 10 keV. Bombardment of the surface with electrons or X-rays of sufficient energy will cause core electrons to be ejected creating singly-ionized, excited atoms. The excited state atom can relax to the ground state through the transition of an electron from a higher energy level to the core vacancy (fig. 22). The energy released during the transition can be transmitted to another electron in the atom, and if this electron then contains more energy than its binding energy, it will be released. The emitted "Auger" electron contains the energy difference between higher energy level and the sum of the core level, and the level of origin of the Auger electron. The most pronounced Auger electron emissions involve KLL, LMM, MNN, NOO, MMM, and OOO transitions. Auger spectra for most elements can be found in literature [ref. 32]. The MMM emission for Cu and the NOO emission for Pb were used for determination of surface coverage of the elements in this investigation [ref. 33]. The notation KLL corresponds to a K core level vacancy filled by a higher energy L level electron and the resulting Auger emission of another L level electron. Auger electron spectroscopy has the ability to detect all elements of higher atomic number than helium.

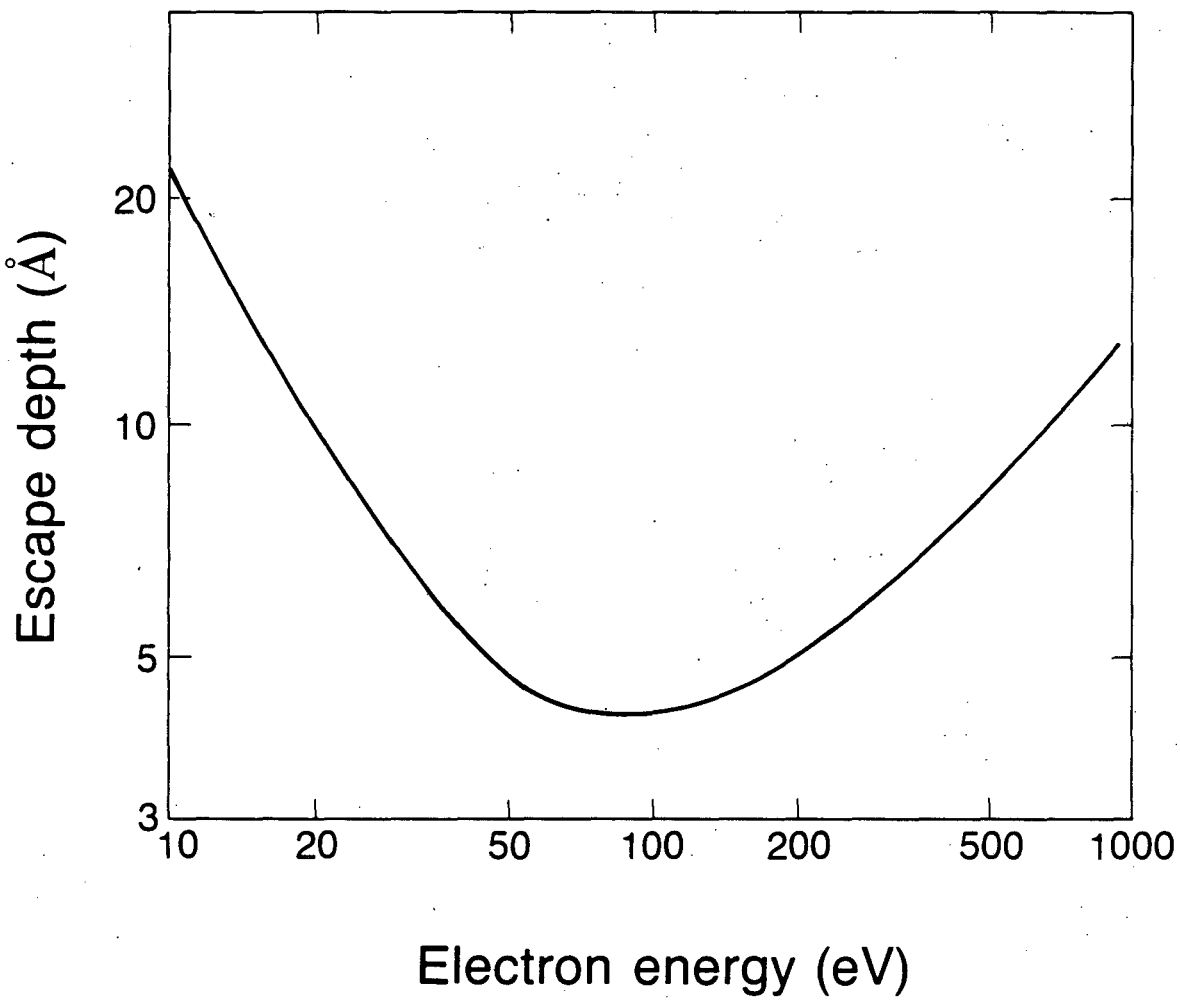

XBL 847-10696

Fig. 21. Universal escape depth curve for electrons [Ref. 31].

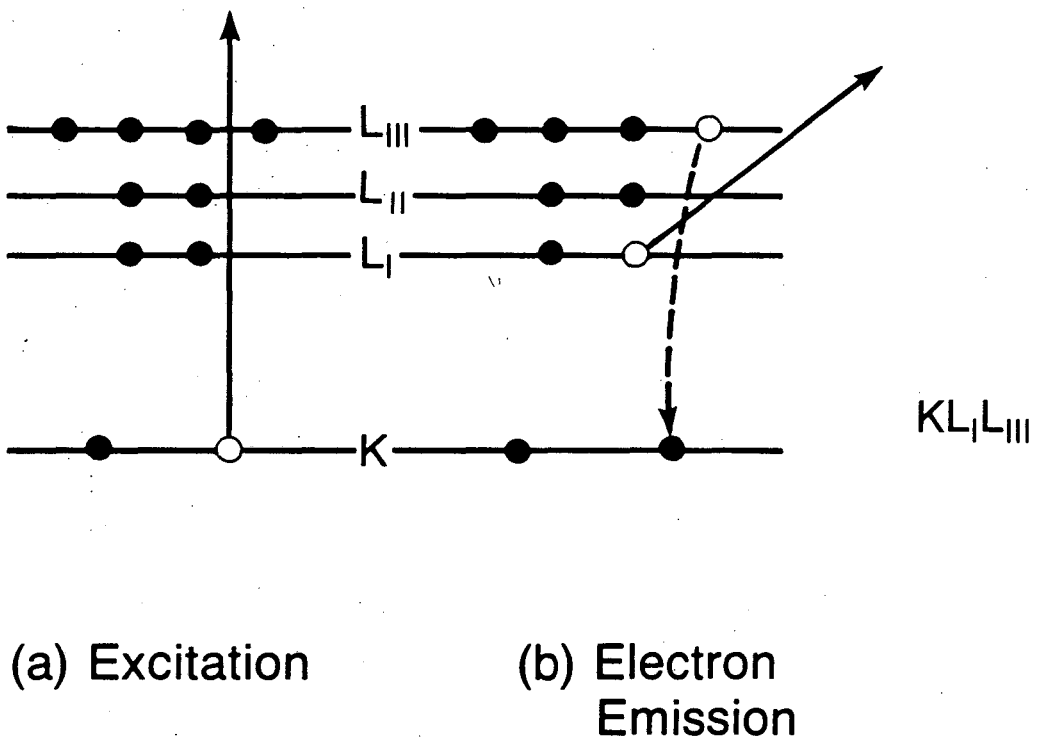

Fig. 22. Schematic of a KLL Auger electron emission.

The surface coverage of islands was calculated from AES measurements. It was assumed that the island height was greater than the escape depth of Auger emissions of the copper and lead atoms. With this assumption the measured Auger emissions were a superposition of emissions from the lead surface and copper surface. The surface coverage was calculated from the relative intensities of the measured Auger peaks weighted by a relative sensitivity factor.

$$\theta(Pb) = \frac{pp(Pb)*sens(Pb)}{pp(Pb)*sens(Pb) + pp(cu)*sens(Cu)}$$

Where $\theta(Pb)$ is the fraction of copper covered by lead, pp(Pb) is the measured peak-to-peak height of the lead Auger emission, pp(Cu) is the peak-to-peak height of the copper Auger emission, sens(Pb) is the sensitivity of the lead Auger emission, and sens(Cu) is the sensitivity of the copper Auger emission. The peak-to-peak heights measured from a copper surface and a lead surface under the same operating conditions were used for the sensitivity factors.

7. APPENDIX B. Ellipsometry

Ellipsometry can be used to measure the change in polarization of light. The changes in polarization occur from the interaction of the light with a reflecting surface. The polarization after a reflection is a function of the initial light polarization, light wavelength, and substrate optical properties. With knowledge of the initial polarization and wavelength, results of ellipsometric measurements can be interpreted to determine the optical properties of the reflecting surface. Compositional and/or morphological information can be obtained from the optical properties. A detailed discussion of the theoretical aspects of ellipsometry can be found in literature [refs. 22,34]. Following is a general discussion of the nomenclature and some optical models. Light as an electromagnetic wave can be described in terms of the orientation of the electric vector. One can decompose the electric wave into two orthogonal components. The two orthogonal components can be characterized by a relative phase relationship and a relative amplitude. The plane of incidence formed by the incident and reflected light path serves as a plane of reference. Linearly polarized light with its electric vector parallel to the plane of incidence is commonly termed "p" polarized. Linearly polarized light perpendicular to the plane of incidence is defined as "s" polarized light (fig. 23). The relative phase change and the relative amplitude change between the p and s components due to reflection can be described by the parameters delta and psi. Delta is defined by the difference between the relative phase of P and S components of the incident light and the relative phase of the reflected light. ψ is defined by

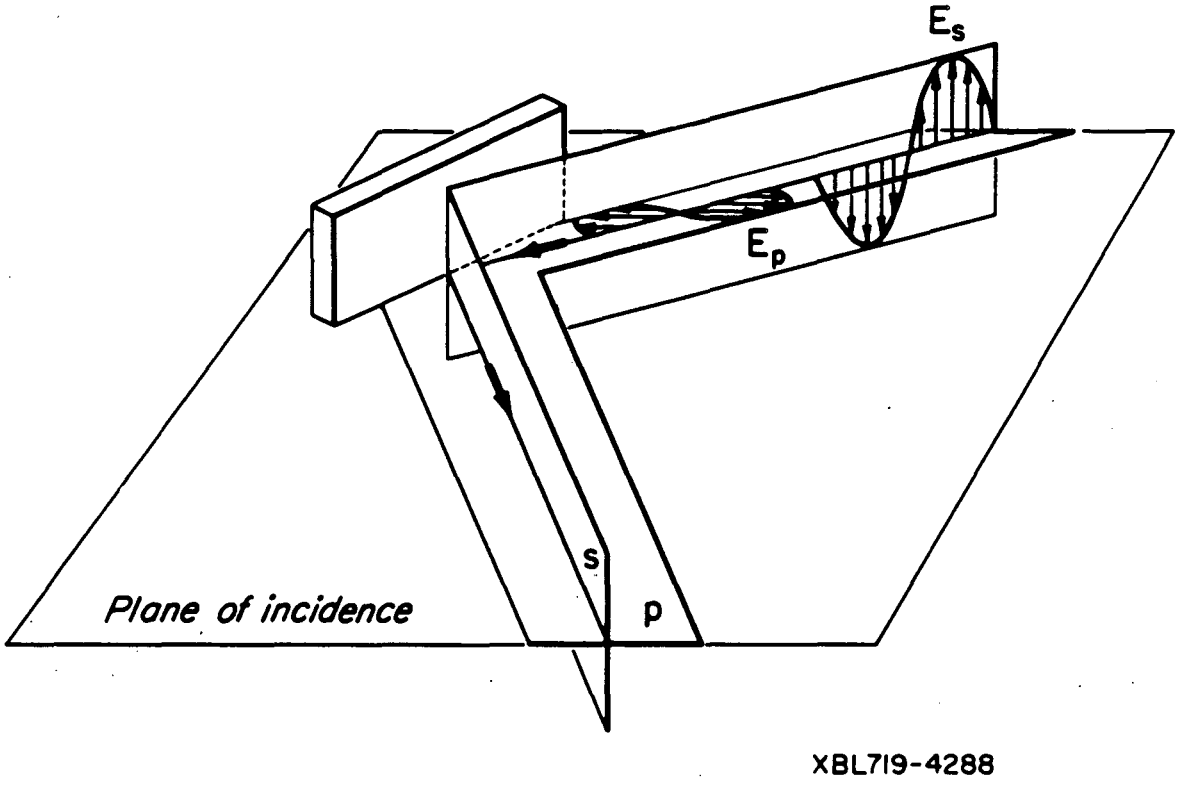

Fig. 23. Electric wave component of an electromagnetic wave decomposed into two orthogonal components s and p.

$$\frac{|E_p|}{|E_s|} = \tan\psi$$

where $|E''|$ is the reflected amplitude and $|E|$ is the incident amplitude of the electric wave. Δ and Ψ are parameters commonly reported from ellipsometric measurements.

The ellipsometer arrangement used here is the polarizer-compensator-sample-analyzer (PCA or PCSA) (fig. 6) [refs. 22,34]. The PCSA arrangement is a null ellipsometer. The compensator produces a quarter wave phase change between its fast and slow axes. The compensator is positioned with the fast axis orientated at ±45° from the plane of incidence. The polarized light becomes elliptically polarized with a phase difference between the p and s components. The p and s amplitudes become equal. At the proper orientation of the polarizer, the phase difference between the p and s component is such that upon reflection from the sample surface, the light is linearly polarized. The linearly polarized reflected light can be extinguished by placing the analyzer at a perpendicular azimuth to the light. The reflected linear polarized light has an orientation determined from the change in relative amplitude of the P and S components. The effective azimuth of the polarizer is related to delta and the effective azimuth of the analyzer is related to psi, Table 4 [ref. 22].

Table 4. Derivation of psi and delta from azimuths of the polarizer, quarter wave retarder, and analyzer [ref. 22].

Zone	Range of Polarizer Transmission Azimuth p	Compensator Fast Axis Azimuth q	Range of Analyzer Transmission Azimuth a	ψ	Δ
A-1	0-45	45	90-180	180-a	90-2p
A-2	45-90	135	90-180	180-a	2p-90
A-3	90-135	45	0-90	a	270-2p
A-4	135-180	135	0-90	a	2p-270
B-1	0-45	135	0-90	a	90+2p
B-2	45-90	45	0-90	a	270-2p
B-3	90-135	135	90-180	180-a	2p-90
B-4	135-180	45	90-180	180-a	450-2p
C-1	0-45	45	0-90	a	270-2p
C-2	45-90	135	0-90	a	90+2p
C-3	90-135	45	90-180	180-a	450-2p
C-4	135-180	135	90-180	180-a	2p-90
D-1	0-45	135	90-180	180-a	270+2p
D-2	45-90	45	90-180	180-a	450-2p
D-3	90-135	135	0-90	a	90+2p
D-4	135-180	45	0-90	a	630-2p

8. APPENDIX C. Program 4ZONE

The program "4ZONE" has been developed to perform four separate spectral scans at the four different zones in which the measurements lie. The program is a modifiction of the data collection program "SEV002" written by J.C. Farmer [ref. 28]. Spectral data are stored in four files with the manually adjusted polarizer, analyzer, and compensator azimuths and general information pertaining to the series of scans. This program records the Faraday cell current and the monochromator position. Monochromator position is determined from the number of pulses following an index pulse of a encoder attached to the monochromator shaft. Analog to digital conversions occur at the maximum possible speed and are averaged over the entire duration between the monochromator encoder pulses. The interference filter rotates twice during the spectral scan of each zone. One rotation is used to move the polarizer, compensator, and analyzer to the proper positions for the zone to be scanned, the second rotation is used for the data collection within the zone. Computer controlled stepping motors adjust the azimuths of the compensator, analyzer, and polarizer to positions in the new zone which correspond to the initial null position found at the beginning of the program. The following equations relate the positions of polarizer, compensator, and analyzer for each zone to the original null position.

ZONE 1

Initial null position found by a subroutine of 4ZONE which minimizes the photomultiplier current and then minimizes the Faraday cell current. The polarizer and analyzer are positioned with stepping motors under control of the running program. The compensator is located at an azimuth of 135.

p(1) = p(null)

c(1) = 45°

a(1) = a(null)

ZONE 2

p(2) = p(null) + 90°

c(2) = 45°

a(2) = - a(null)

ZONE 3

p(3) = - p(null)

c(3) = 135°

a(3) = - a(null)

ZONE 4

p(4) = 90° - p(null)

c(4) = 135°

a(4) = a(null)

The following is a demonstration of the computer prompts and operator response for a four zone data acquisition session.

```
.RUN 4ZONE

DO YOU WANT TO REVIEW ENCODER WAVELENGHT CALIBRATION PARAMETERS (Y/N)N

INSERT DATA STORAGE DISK, THEN 'RETURN'.

DO YOU WANT TO ADJUST THE SCAN RATE(Y/N)?N

STEADY SCAN RATE ESTABLISHED.  SCAN RATE =131

IS SETUP INFO TO BE (A)ENTERED FROM KEYBOARD OF (B)READ FROM OLD DATA FILE?A

LAMP PARAMETERS:
TYPE(A2/XE,ETC.) =XE
SERIAL NO.(A18) =1A7-20
LAMP VOLTAGE(I3/VOLTS) =15
LAMP CURRENT(I2/AMPS) =6

PHOTOMULTIPLIER PARAMETERS:
MODEL(A20) =HAMAMATSU R928
DYNODE VOLTAGE(I4/VOLTS) =1100

FARADAY CELL CONTROLLER PARAMETERS:

POLARIZER CHANNEL
PHASE(I3/POT SETTING) =702
GAIN(I3/POT SETTING) = 999
AMPLITUDE(I3/POT SETTING) =900
TIME CONSTANT(I3/MILLISECONDS) =10

ANALYZER CHANNEL
PHASE(I3/POT SETTING) =966
GAIN(I2/POT SETTING) = 999
AMPLITUDE(I3/POT SETTING) =900
TIME CONSTANT(I3/MILLISECONDS) =10

GALVANOMETER AMPLIFIER PARAMETERS:

POLARIZER CHANNEL
GAIN(I5) =10
TIME CONSTANT(I5/MILLISECONDS) =1

ANALYZER CHANNEL
GAIN(I5) =10
TIME CONSTANT(I5/MILLISECONDS) =1

NAME(A40) =MIKE ARMSTRONG

DATE(I2-A3-I2/DAY-MONTH-YEAR) =04-JUN-84

LAMP OPERATIONAL LIFE(I5/HOURS) =488

EXPERIMENT IDENTIFICATION(A40) =DEMONSTRATION
```

```
INITIAL POSITIONS
POL = 90.00
ANA = 90.00
CMP = 0.00
      ANY CHANGES?N

ANALOG/DIGITAL CONVERTOR PRESET PARAMETERS:
POL. INPUT CH. = 0
ANA. INPUT CH. = 1
ADC GAIN       = 3

DO YOU WANT TO CHANGE THESE(Y/N)?N

HOW MANY SPECTRAL SCANS ARE TO BE AVERAGED(I5)?1
   BASE FILE NAME TO BE USED(A4) ?DEMO
Set monochromator to prefered wavelenght.
Make sure all necessary instruments are on and
the F. C. controller in closed circut.
Hit return key when ready.


IS SETUP INFORMATION TO BE OUTPUT (A)TO CRT, (B)TO PRINTER, OR (C)NOT AT ALL?A

ENTER 'G' AND 'RETURN' FOR SPECTRA COLLECTION.G

SPECTRA BEING COLLECTED............

  EACH POINT AN AVERAGE OF: 205. CHANNEL SCANS

  EACH POINT AN AVERAGE OF: 200. CHANNEL SCANS

  EACH POINT AN AVERAGE OF: 205. CHANNEL SCANS

  EACH POINT AN AVERAGE OF: 200. CHANNEL SCANS
PAUSE — HIT RETURN AFTER OPENING CONTROL LOOP

DO YOU WANT TO PLOT SPECTRA(Y/N)?Y
```

```
RANGES OF DATA TO BE PLOTTED:
     MAXIMUM WAVELENGHT(ANGSTROMS) =        7371
     MINIMUM                       =        3507
     MAXIMUM POLARIZER CURRENT     =       0.000
     MINIMUM                       =   -1780.000
     MAXIMUM ANALYZER CURRENT      =     450.000
     MINIMUM -                     =   -1234.000

DO YOU WANT TO CHANGE THEASE(Y/N)?N

     PLOTTING MENU FOR REFRACTIVE INDEX DATA:
          (1) POLARIZER CURRENT(ADCU,Y-AXIS) VS ENCODER COUNT(X-AXIS)
          (2) ANALYZER CURRENT(ADCU,Y-AXIS) VS ENCODER COUNT(X-AXIS)
          (3) POLARIZER CURRENT(ADCU,Y-AXIS) VS WAVELENGHT(X AXIS)
          (4) ANALYZER CURRENT(ADCU,Y-AXIS) VS WAVELENGHT(X-AXIS)
          (5) ANALYZER CURRENT(Y-AXIS) VS POLARIZER CURRENT(X-AXIS)

YOUR CHOICE(1,2,3,4,OR 5)?3

HOW MANY SCALE DIVISIONS DO YOU WANT FOR THE X-COORDINATE(I2)?2

HOW MANY SCALE DIVISIONS DO YOU WANT FOR THE Y-COORDINATE(I2)?3

IS THE GRAPH TO BE LABELED(Y/N)?Y
```

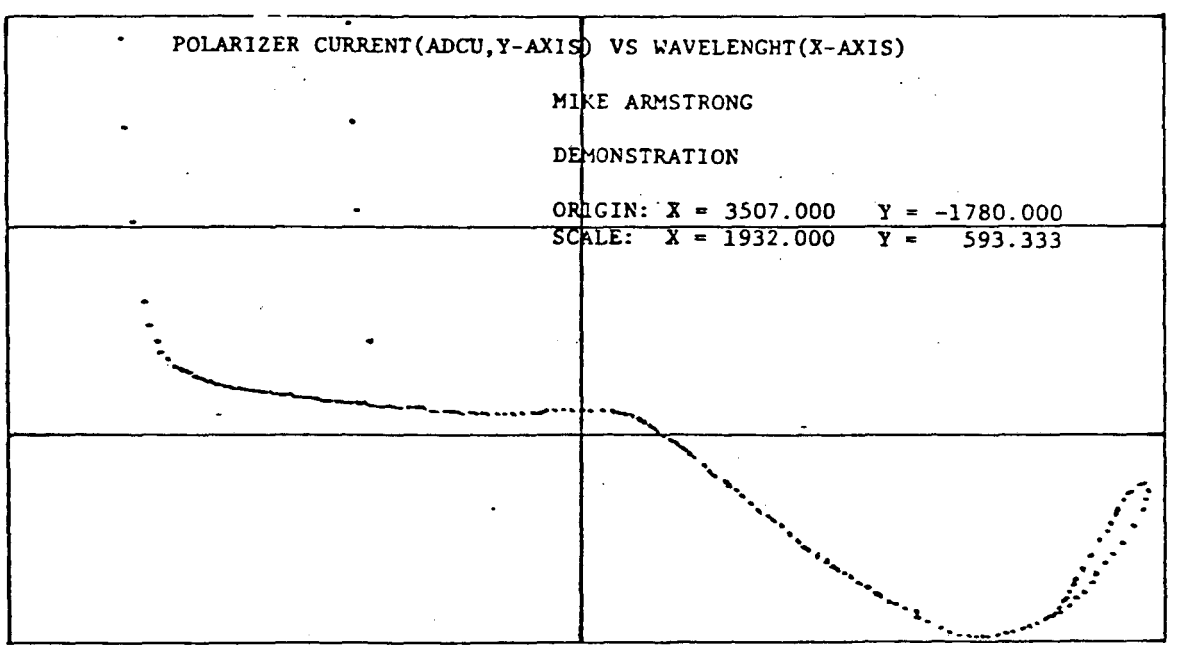

```
E ANY ADDITIONAL PLOTS WANTED(Y/N)?N
 ANY NUMERIC OUTPUT DESIRED(Y/N)?N
 THE PROGRAM TO BE EXECUTED AGAIN(Y/N)?N
OP --
```

```
      PROGRAM Z4ZONE
C*********************************************************************
C     OBJECTIVE: TO COORDINATE THE ACTUAL DATA ACQUISITION DURING AN
C                ELLIPSOMETRIC SPECTRAL SCAN WITH OPERATOR REVIEW OF
C                THE RAW DATA.  THIS IS THE MAIN DATA COLLECTION
C                ROUTINE. PERFORMS A 4 ZONE SPECTRAL SCAN WITH EACH
C                ZONE SPECTRAL DATA RECORDED IN SEPERATE FILES.
C
C     PROGRAM WRITTEN BY JOSEPH C. FARMER IN SPRING 1981 LBL-MMRD
C     MODIFIED FROM SEV002 BY MICHAEL ARMSTRONG MAY 1983
C
C*********************************************************************
      COMMON/A/NAVG(400),POL(400),ANA(400)
      COMMON/B/NRATE,NSCAN,IPOL,IANA
      COMMON/E/NAMEOP(20),ID(20)
      COMMON/F/LMPTYP,LMPSER(10),LMPVLT,LMPAMP
      COMMON/G/IPMTYP(10),IPMTDV
      COMMON/H/IPHASP,IPHASA,IGAINP,IGAINA,IAMPLP,IAMPLA,ITIMEP,ITIMEA
      COMMON/I/IGAGP,IGAGA,IGATP,IGATA
      COMMON/J/NWL,NPOL,NCMP,NANA
      COMMON/K/IHRSO,IMINO,ISECO,ITICO,IHRSF,IMINF,ISECF,ITICF
      COMMON/L/IDAY,IMON(3),IYRS,LMPHRS
      COMMON/M/IWAVE(400)
      COMMON/N/ICHAN,IBLOCK,IFLAG,IBUFF(256)
      COMMON/O/NPASS
      COMMON/STATUS/ISTAT(16)
      COMMON/TITLE/NTITLE(5,30),NWORD(2,21)
      COMMON/MODE/MODEO,MODEI,FACTOR
        COMMON/MOVER/IAMOV,IJMOV
        COMMON/OP/FILENM(4)
      NPASS=1
C*****THE ENCODER COUNT IS CONVERTED TO WAVELENGTH.*******************
      CALL WLCALC
C*****THE GRAPHICS TITLES ARE READ FROM "DY1:TITLE.DAT".***************
      MODEO=1
      CALL TITLE
      TYPE 10
   10 FORMAT(/,'$ INSERT DATA STORAGE DISK, THEN "RETURN".')
      ACCEPT 20,NWAIT
   20 FORMAT(A1)
C*****THE FOURTH CHANNEL OF THE ADAC MODEL 1604/OPI COUNTER CARD IS ***
C     READ AT VARIOUS TIMES TO ASSURE THAT THE RATE OF ROTATION OF
C     THE FILTER DISC(SPECTRAL SCANNING RATE) IS CONSTANT.  PROGRAM
C     EXECUTION IS DELAYED UNTIL A SPECIFIED STABILITY CRITERIA IS
C     MET.  CHANNEL 4 OF THIS COUNTER CARD IS WIRE WRAPPED TO
C     OPERATE IN THE FREQUENCY MODE; THE FREQUENCY OF THE ENCODER
C*****GENERATED PULSES IS MEASURED BY THIS CHANNEL.*******************
   30 CALL RATE
      NSAVE=NRATE
C*****SETUP INFORMATION IS EITHER READ FROM A PREVIOUS EXPERIMENTAL ****
C     DATA FILE OR INPUT FROM THE VT55 KEYBOARD BY THE OPERATOR,
C     DEPENDING UPON THE OPERATOR'S RESPONSE AT THIS POINT.
  100 TYPE 110
  110 FORMAT(/,'$ IS SETUP INFO TO BE (A)ENTERED FROM KEYBOARD
     C OR (B)READ FROM OLD DATA FILE? ')
      ACCEPT 20,IF1
      IF(IF1.NE.1HA.AND.IF1.NE.1HB)GOTO 100
      IF(IF1.NE.1HA)GOTO 120
C*****THIS SUBROUTINE ALLOWS THE OPERATOR TO INPUT THE SETUP **********
C     INFORMATION FROM THE KEYBOARD.
```

```
      CALL NEWSET
      GOTO 130
  120 CONTINUE
C*****THIS SUBROUTINE ACCESSES AN OLD DATA FILE SPECIFIED BY THE ******
C     OPERATOR TO REASSIGN OLD SETUP VALUES TO THE CURRENT
C     EXPERIMENT.
      CALL INPUT
      NRATE=NSAVE
  130 CONTINUE
C*****SOME PARAMETERS MUST BE ENTERED FROM THE KEYBOARD SINCE *********
C     THEY WILL PROBABLY BE CHANGED FROM ONE SPECTRAL SCAN TO
C     ANOTHER(FOR EXAMPLE MANUAL AZIMUTH SETTINGS).  SUBROUTINE
C     "RESET" ALLOWS FOR THIS.
      CALL RESET
        NMV=(-NCMP)/2
        IAMOV=67
        IJMOV=NMV
        CALL MOVE
        NMV=0
        IAMOV=67
        IJMOV= 2250
        CALL MOVE
        NCMP=13500
        TYPE 9921
9921    FORMAT('$    BASE FILE NAME TO BE USED(A4) ? ')
        ACCEPT 9922,FILENM(2)
        FILENM(1)='DY10'
9922    FORMAT(A4)
C*****The analyser and polariser are mechanically rotated to  *********
C     get a null with the step motor controller
        CALL NULL(JPCNT,JACNT,J12)
        NANA=NANA+JACNT*100
        NPOL=NPOL+JPCNT*100
D       TYPE *,NANA,NPOL
        IF(NPOL.LT.0)NPOL=18000+NPOL
C*****THE OPERATOR CAN SPECIFY THE TYPE OF OUTPUT DESIRED FOR *********
C     THE SETUP INFORMATION.
  200 TYPE 210
  210 FORMAT(/,'$ IS SETUP INFORMATION TO BE OUTPUT (A)TO CRT,
     C (B)TO PRINTER, OR (C)NOT AT ALL? ')
      ACCEPT 20,IF2
      IF(IF2.NE.1HA.AND.IF2.NE.1HB.AND.IF2.NE.1HC)GOTO 200
      IF(IF2.EQ.1HC)GOTO 230
      IF(IF2.NE.1HA)GOTO 220
C*****SETUP INFORMATION IS DISPLAYED ON THE CRT.**********************
      CALL T1INFO
      GOTO 230
  220 CONTINUE
C*****SETUP INFORMATION IS SENT TO THE LINE PRINTER.******************
      CALL P1INFO
  230 CONTINUE
  400 TYPE 410
  410 FORMAT(/,'$ ENTER "G" AND "RETURN" FOR SPECTRA COLLECTION. ')
      ACCEPT 20,IF3
      IF(IF3.NE.1HG)GOTO 400
      TYPE 411
  411 FORMAT(/,'  SPECTRA BEING COLLECTED..........')
        FILENM(3)='0001'
      CALL EDATA
        CALL OUTPUT
```

```
      IPMV=(NPOL-9000)/IABS(NPOL-9000)*(-4500)
      IAMV=9000-NANA
      NPOL=NPOL+IPMV*2
      NANA=NANA+IAMV*2
      IJMOV=IPMV
      IAMOV=80
      CALL MOVE
      IJMOV=IAMV
      IAMOV=65
      CALL MOVE
      FILENM(3)='0002'
      CALL EDATA
      CALL OUTPUT
      IAMOV=67
      IJMOV=4500
      CALL MOVE
      NCMP=4500
      IF(NPOL.GT.9000) IPMV=13500-NPOL
      IF(NPOL.LE.9000)IPMV=4500-NPOL
      NPOL=NPOL+IPMV*2
      IAMOV=80
      IJMOV=IPMV
      CALL MOVE
      FILENM(3)='0003'
      CALL EDATA
      CALL OUTPUT
      IPMV=(NPOL-9000)/IABS(NPOL-9000)*(-90)*50
      IAMV=9000-NANA
      NPOL=NPOL+IPMV*2
      NANA=NANA+IAMV*2
      IJMOV=IPMV
      IAMOV=80
      CALL MOVE
      IJMOV=IAMV
      IAMOV=65
      CALL MOVE
      FILENM(3)='0004'
      CALL EDATA
      CALL OUTPUT
      PAUSE 'HIT RETURN AFTER OPENING CONTROL LOOP'
      IJMOV=-2250
      IAMOV=67
      CALL MOVE
      IPMV=(9000-NPOL)/2
      IAMV=(9000-NANA)/2
      IJMOV=IPMV
      IAMOV=80
      CALL MOVE
      IJMOV=IAMV
      IAMOV=65
      CALL MOVE
C*****THE REQUIRED DATA ACQUISITION TIME FOR THE SPECTRAL SCAN IS *****
C     EITHER DISPLAYED ON THE CRT OR OUTPUT ON THE LINE PRINTER.
      IF(IF2.EQ.1HC)GOTO 630
      IF(IF2.NE.1HA)GOTO 620
      CALL T1TIME
      GOTO 630
  620 CONTINUE
      CALL P1TIME
  630 CONTINUE
```

```
C*****IF DESIRED, THE SPECTRAL SCAN IS DISPLAYED ON THE VT55 **********
C     TERMINAL IN GRAPHICAL FORM.
  700 TYPE 710
  710 FORMAT(/,'$ DO YOU WANT TO PLOT SPECTRA(Y/N)? ')
      ACCEPT 20,IF4
      IF(IF4.NE.1HY.AND.IF4.NE.1HN)GOTO 700
      IF(IF4.EQ.1HN)GOTO 720
      CALL PLOT
  720 CONTINUE
C*****DEPENDING ON THE OPERATOR'S RESPONSE, VARIOUS COMBINATIONS ******
C     OF NUMERICAL OUTPUT CAN BE GENERATED(EITHER CRT DISPLAY OR
C     HARDCOPY FROM THE LINE PRINTER.
820   TYPE 890
  890 FORMAT(/,'$ IS ANY NUMERIC OUTPUT DESIRED(Y/N)? ')
      ACCEPT 20,IF6
      IF(IF6.NE.1HY.AND.IF6.NE.1HN)GOTO 820
      IF(IF6.EQ.1HN)GOTO 960
  900 TYPE 910
  910 FORMAT(/,5X,'NUMERIC OUTPUT MENU:',
     C         /,10X,'(A)HARDCOPY OF SETUP INFO. ONLY',
     C         /,10X,'(B)HARDCOPY OF SETUP INFO. AND PLOTTED DATA PTS.',
     C         /,10X,'(C)CRT DISPLAY OF SETUP INFO. ONLY',
     C         /,10X,'(D)CRT DISPLAY OF SETUP INFO. AND PLOTTED DATA
     C PTS.', /,10X,'(E)NONE OF THE ABOVE')
      TYPE 920
  920 FORMAT(/,'$     YOUR CHOICE IS: ')
      ACCEPT 20,IF6
      IF(IF6.NE.1HA.AND.IF6.NE.1HB.AND.IF6.NE.1HC.AND.IF6.NE.1HD
     C.AND.IF6.NE.1HE)GOTO 900
      IF(IF6.EQ.1HE)GOTO 960
      IF(IF6.NE.1HA)GOTO 930
      CALL P1INFO
      CALL P1TIME
  930 CONTINUE
      IF(IF6.NE.1HB)GOTO 940
      CALL P1INFO
      CALL P1TIME
      DO 934 IPAGE=1,4
      PRINT 931,IPAGE
  931 FORMAT(///,5X,'DATA(ADCU) FROM POLARIZER AND ANALYZER CHANNELS
     C AS A FUNCTION OF WAVELENGTH(ANGSTROMS)...PAGE ',I1,
     C        ///,2(5X,'INDEX',5X,'WL',3X,'NAVG',7X,'POL',7X,'ANA'))
      DO 932 I=1,50
      I1=(IPAGE-1)*100+I
      I2=I1+50
  932 PRINT 933,I1,IWAVE(I1),NAVG(I1),POL(I1),ANA(I1),I2,IWAVE(I2),
     CNAVG(I2),POL(I2),ANA(I2)
  933 FORMAT(2(5X,I5,2X,I5,2X,I5,3X,F7.0,3X,F7.0))
  934 PRINT 935
  935 FORMAT(////////)
  940 CONTINUE
      IF(IF6.NE.1HC)GOTO 950
      CALL T1INFO
      CALL T1TIME
  950 CONTINUE
      IF(IF6.NE.1HD)GOTO 960
      CALL T1INFO
      CALL T1TIME
      TYPE 951
  951 FORMAT(//,5X,'RAW DATA FROM SPECTRAL SCAN',//)
```

```
      DO 952 I=1,400
  952 TYPE 953,I,IWAVE(I),NAVG(I),POL(I),ANA(I)
  953 FORMAT(5X,'I = ',I3,5X,'WL = ',I5,5X,'NAVG = ',I3,5X,'POL = ',
     CF7.0,5X,'ANA = ',F7.0)
  960 CONTINUE
C*****THE OPERATOR HAS THE OPTION OF REPEATING PROGRAM EXECUTION.******
 1000 TYPE 1010
 1010 FORMAT(/,'$ IS THE PROGRAM TO BE EXECUTED AGAIN(Y/N)? ')
      ACCEPT 20,IF7
      IF(IF7.NE.1HY.AND.IF7.NE.1HN)GOTO 1000
      NPASS=NPASS+1
      IF(IF7.EQ.1HY)GOTO 30
      STOP
      END

      SUBROUTINE RATE
C*********************************************************************
C     OBJECTIVE: MAKE TWO "AVERAGED" DETERMINATIONS OF THE ROTATION
C                RATE OF THE FILTER DISK(SPECTRAL SCAN RATE) VIA
C                CHANNEL 4 OF THE ADAC 1604/OPI COUNTER CARD WHICH
C                IS WIRE WRAPPED IN THE FREQUENCY MODE.  THESE TWO
C                RATES OF ROTATION ARE MADE AT A TIME INTERVAL
C                DETERMINED BY THE SUBROUTINE "DELAY"(15 SECONDS).
C                IF THE TWO RATES ARE IDENTICAL, THE SCAN RATE IS
C                DETERMINED TO BE STABLE(FREE OF "CHATTER", ETC.)
C                AND PROGRAM CONTROL IS RETURNED TO THE MAIN
C                PROGRAM "SEV001".
C*********************************************************************
      COMMON/B/NRATE,NSCAN,IPOL,IANA
   10 TYPE 20
   20 FORMAT(/,'$ DO YOU WANT TO ADJUST THE SCAN RATE(Y/N)? ')
      ACCEPT 30,MRATE
   30 FORMAT(A1)
      IF(MRATE.NE.1HY.AND.MRATE.NE.1HN)GOTO 10
      IF(MRATE.NE.1HY)GOTO 85
      TYPE 40
   40 FORMAT(/,'$ ADJUST THE SPECTRAL SCANNER SPEED, THEN "RETURN".')
      ACCEPT 50,IWAIT
   50 FORMAT(A1)
   60 ISUM0=0
      DO 70 I=1,3
   70 ISUM0=ISUM0+IPEEK("164406)
      CALL DELAY
      ISUM1=0
      DO 80 I=1,3
   80 ISUM1=ISUM1+IPEEK("164406)
      IF(ISUM0.NE.ISUM1)GO TO 60
   85 NRATE=IPEEK("164406)
      TYPE 90,NRATE
   90 FORMAT(/,'  STEADY SCAN RATE ESTABLISHED.  SCAN RATE = ',I5)
      RETURN
      END

      SUBROUTINE DELAY
C*********************************************************************
C     OBJECTIVE: TO GENERATE A 15 SECOND TIME DELAY FOR SUBROUTINE
C                "RATE".
C*********************************************************************
      INTEGER*4 ITIME
   10 CALL GTIM(ITIME)
```

```
      CALL CVTTIM(ITIME,IHRS,IMIN,ISEC,ITIC)
      ISEC0=ISEC
      IF(ISEC0.GT.44)GOTO 10
   20 CALL GTIM(ITIME)
      CALL CVTTIM(ITIME,IHRS,IMIN,ISEC,ITIC)
      ISECF=ISEC
      IF(ISECF.EQ.ISEC0+15)RETURN
      GOTO 20
      END
```

```
        SUBROUTINE MOVE
        COMMON/MOVER/ IAMOV,IJMOV
        I=IJMOV
        IDIR=0
        IF(IAMOV.EQ.65)GOTO 30
        IF(IAMOV.EQ.80)GOTO 40
        IF(IAMOV.EQ.67)GOTO 50
30      IF(I.LT.0)IDIR=2048
        I=IABS(I)
32      IF(IPEEK("164502).GT.0)GOTO 32
        IF(I.GT.2047)GOTO 31
        I=I+IDIR
        CALL IPOKE("164502,I)
33      IF(IPEEK("164502).GT.0)GOTO 33
        GOTO 10
31      I=I-2047
        IT=2047+IDIR
        CALL IPOKE("164502,IT)
        GOTO 32
40      IF(I.GT.0)IDIR=2048
        I=IABS(I)
42      IF(IPEEK("164506).GT.0) GOTO 42
        IF(I.GT.2047)GOTO 41
        I=I+IDIR
        CALL IPOKE("164506,I)
43      IF(IPEEK("164506).GT.0) GOTO 43
        GOTO 10
41      I=I-2047
        IT=IDIR+2047
        CALL IPOKE("164506,IT)
        GOTO 42
50      IF(I.LT.0)IDIR=2048
        I=IABS(I)
52      IF(IPEEK("164504).GT.0)GOTO 52
        IF(I.GT.2047)GOTO 51
        I=I+IDIR
        CALL IPOKE("164504,I)
53      IF(IPEEK("164504).GT.0)GOTO 53
        GOTO 10
51      I=I-2047
        IT=IDIR+2047
        CALL IPOKE("164504,IT)
        GOTO 52
10      RETURN
100     FORMAT(A1,I5)
200     FORMAT(T10,A1,2X,I5)
        END
```

```
      SUBROUTINE INPUT
C*********************************************************************
C     OBJECTIVE: TO READ THE SETUP INFORMATION AND SPECTRAL SCAN DATA
C                FROM ANY FLOPPY DISK FILE SPECIFIED BY THE OPERATOR
C                AND CREATED BY SUBROUTINE "OUTPUT".
C*********************************************************************
      COMMON/A/NAVG(400),POL(400),ANA(400)
      COMMON/B/NRATE,NSCAN,IPOL,IANA
      COMMON/E/NAMEOP(20),ID(20)
      COMMON/F/LMPTYP,LMPSER(10),LMPVLT,LMPAMP
      COMMON/G/IPMTYP(10),IPMTDV
      COMMON/H/IPHASP,IPHASA,IGAINP,IGAINA,IAMPLP,IAMPLA,ITIMEP,ITIMEA
      COMMON/I/IGAGP,IGAGA,IGATP,IGATA
      COMMON/J/NWL,NPOL,NCMP,NANA
      COMMON/K/IHRS0,IMIN0,ISEC0,ITIC0,IHRSF,IMINF,ISECF,ITICF
      COMMON/L/IDAY,IMON(3),IYRS,LMPHRS
      COMMON/M/IWAVE(400)
      COMMON/N/ICHAN,IBLOCK,IFLAG,IBUFF(256)
      REAL*4 BDLK(2),NAME(20)
      IBLOCK=0
      TYPE 100
  100 FORMAT(/,'$ NAME OF SPECTRA FILE TO BE RETRIEVED = ')
      ACCEPT 200,(NAME(I),I=1,3)
  200 FORMAT(3A4)
      N=IRAD50(12,NAME,BDLK)
      ICHAN=IGETC(I)
      IF(ICHAN.LT.0)STOP 'CANNOT ALLOCATE CHANNEL'
      IF(IFETCH(ICHAN).LT.0)STOP 'FETCH FAIL'
      IF(LOOKUP(ICHAN,BDLK).LT.0)STOP 'BAD LOOKUP'
      DO 10 I=1,256
   10 IBUFF(I)=0
      CALL READ
      DO 20 I=1,20
      NAMEOP(I)=IBUFF(I)
   20 ID(I)=IBUFF(20+I)
      LMPTYP=IBUFF(41)
      DO 30 I=1,9
   30 LMPSER(I)=IBUFF(41+I)
      LMPVLT=IBUFF(51)
      LMPAMP=IBUFF(52)
      IPHASP=IBUFF(54)
      IGAINP=IBUFF(55)
      IAMPLP=IBUFF(56)
      ITIMEP=IBUFF(57)
      IPHASA=IBUFF(58)
      IGAINA=IBUFF(59)
      IAMPLA=IBUFF(60)
      ITIMEA=IBUFF(61)
      IGAGP =IBUFF(62)
      IGATP =IBUFF(63)
      IGAGA =IBUFF(64)
      IGATA =IBUFF(65)
      NRATE =IBUFF(66)
      NSCAN =IBUFF(67)
      IPOL  =IBUFF(68)
      IANA  =IBUFF(69)
      NWL   =IBUFF(70)
      NPOL  =IBUFF(71)
      NCMP  =IBUFF(72)
      NANA  =IBUFF(73)
```

```
      IHRSO =IBUFF(74)
      IHRSF =IBUFF(75)
      IMINO =IBUFF(76)
      IMINF =IBUFF(77)
      ISECO =IBUFF(78)
      ISECF =IBUFF(79)
      ITICO =IBUFF(80)
      ITICF =IBUFF(81)
      IDAY  =IBUFF(82)
      IYRS  =IBUFF(83)
      LMPHRS=IBUFF(84)
      IMON(1)=IBUFF(85)
      IMON(2)=IBUFF(86)
      IMON(3)=IBUFF(87)
      DO 35 I=1,10
   35 IPMTYP(I)=IBUFF(87+I)
      IPMTDV=IBUFF(98)
      CALL READ
      DO 40 I=1,200
   40 POL(I)=IBUFF(I)
      CALL READ
      DO 50 I=1,200
   50 ANA(I)=IBUFF(I)
      CALL READ
      DO 60 I=1,200
   60 POL(I+200)=IBUFF(I)
      CALL READ
      DO 70 I=1,200
   70 ANA(I+200)=IBUFF(I)
      CALL CLOSEC(ICHAN)
      CALL IFREEC(ICHAN)
      RETURN
      END

      SUBROUTINE READ
C*********************************************************************
C     OBJECTIVE: TO ACTUALLY READ THE DATA STORED ON THE FLOPPY DISK
C                INTO BUFFER MEMORY.
C*********************************************************************
      COMMON/N/ICHAN,IBLOCK,IFLAG,IBUFF(256)
      IERROR=IREADW(256,IBUFF,IBLOCK,ICHAN)
      IF(IERROR.LT.0)STOP 'FATAL READ'
      IBLOCK=IBLOCK+1
      RETURN
      END
```

```
      SUBROUTINE OUTPUT
C*********************************************************************
C     OBJECTIVE: TO WRITE THE SETUP INFORMATION AND DATA FROM THE
C                SPECTRAL SCAN INTO ANY FLOPPY DISK FILE SPECIFIED
C                BY THE OPERATOR.
C*********************************************************************
      COMMON/A/NAVG(400),POL(400),ANA(400)
      COMMON/B/NRATE,NSCAN,IPOL,IANA
      COMMON/E/NAMEOP(20),ID(20)
      COMMON/F/LMPTYP,LMPSER(10),LMPVLT,LMPAMP
      COMMON/G/IPMTYP(10),IPMTDV
      COMMON/H/IPHASP,IPHASA,IGAINP,IGAINA,IAMPLP,IAMPLA,ITIMEP,ITIMEA
      COMMON/I/IGAGP,IGAGA,IGATP,IGATA
      COMMON/J/NWL,NPOL,NCMP,NANA
      COMMON/K/IHRSO,IMINO,ISECO,ITICO,IHRSF,IMINF,ISECF,ITICF
      COMMON/L/IDAY,IMON(3),IYRS,LMPHRS
      COMMON/M/IWAVE(400)
      COMMON/N/ICHAN,IBLOCK,IFLAG,IBUFF(256)
        COMMON/OP/FILENM(4)
      REAL*4 DBLK(2),NAME(20)
      IBLOCK=0
      N=IRAD50(12,FILENM,DBLK)
      ICHAN=IGETC(0)
      IF(ICHAN.LT.0)STOP 'CANNOT ALLOCATE CHANNEL'
      IERROR=IENTER(ICHAN,DBLK,0)
      IF(IERROR.LT.0)STOP 'ENTER FAILURE'
      DO 10 I=1,256
   10 IBUFF(I)=0
      DO 20 I=1,20
      IBUFF(I)=NAMEOP(I)
   20 IBUFF(20+I)=ID(I)
      IBUFF(41)=LMPTYP
      DO 30 I=1,9
   30 IBUFF(41+I)=LMPSER(I)
      IBUFF(51)=LMPVLT
      IBUFF(52)=LMPAMP
      IBUFF(54)=IPHASP
      IBUFF(55)=IGAINP
      IBUFF(56)=IAMPLP
      IBUFF(57)=ITIMEP
      IBUFF(58)=IPHASA
      IBUFF(59)=IGAINA
      IBUFF(60)=IAMPLA
      IBUFF(61)=ITIMEA
      IBUFF(62)=IGAGP
      IBUFF(63)=IGATP
      IBUFF(64)=IGAGA
      IBUFF(65)=IGATA
      IBUFF(66)=NRATE
      IBUFF(67)=NSCAN
      IBUFF(68)=IPOL
      IBUFF(69)=IANA
      IBUFF(70)=NWL
      IBUFF(71)=NPOL
      IBUFF(72)=NCMP
      IBUFF(73)=NANA
      IBUFF(74)=IHRSO
      IBUFF(75)=IHRSF
      IBUFF(76)=IMINO
      IBUFF(77)=IMINF
```

```
      IBUFF(78)=ISECO
      IBUFF(79)=ISECF
      IBUFF(80)=ITICO
      IBUFF(81)=ITICF
      IBUFF(82)=IDAY
      IBUFF(83)=IYRS
      IBUFF(84)=LMPHRS
      IBUFF(85)=IMON(1)
      IBUFF(86)=IMON(2)
      IBUFF(87)=IMON(3)
      DO 35 I=1,10
   35 IBUFF(87+I)=IPMTYP(I)
      IBUFF(98)=IPMTDV
      CALL WRITE
      CALL IWAIT(ICHAN)
      DO 40 I=1,200
   40 IBUFF(I)=POL(I)
      CALL WRITE
      CALL IWAIT(ICHAN)
      DO 50 I=1,200
   50 IBUFF(I)=ANA(I)
      CALL WRITE
      CALL IWAIT(ICHAN)
      DO 60 I=1,200
   60 IBUFF(I)=POL(I+200)
      CALL WRITE
      CALL IWAIT(ICHAN)
      DO 70 I=1,200
   70 IBUFF(I)=ANA(I+200)
      CALL WRITE
      CALL IWAIT(ICHAN)
      CALL CLOSEC(ICHAN)
      CALL IFREEC(ICHAN)
      RETURN
      END


      SUBROUTINE WRITE
C*********************************************************************
C     OBJECTIVE: THIS SUBROUTINE ACTUALLY WRITES THE DATA STORED IN THE
C                BUFFER MEMORY TO THE SPECIFIED DISK FILE.
C*********************************************************************
      COMMON/N/ICHAN,IBLOCK,IFLAG,IBUFF(256)
      EXTERNAL FINISH
      IERROR=IWRITF(256,IBUFF,IBLOCK,ICHAN,IAREA,FINISH)
      IF(IERROR.LT.0)STOP 'FATAL WRITE'
      IBLOCK=IBLOCK+1
      RETURN
      END


      SUBROUTINE FINISH
      COMMON/N/ICHAN,IBLOCK,IFLAG,IBUFF(256)
      IFLAG=IFLAG-1
      RETURN
      END
```

```
      SUBROUTINE RESET
C*********************************************************************
C     OBJECTIVE: TO ALLOW THE OPERATOR TO CHANGE ONLY THOSE SETUP
C                PARAMETERS WHICH ARE TYPICALLY CHANGED FROM ONE
C                SPECTRAL SCAN TO ANOTHER.  THIS MODIFYS SETUP
C                INFORMATION READ FROM OLD DATA FILES TO MAKE IT
C                APPLICABLE TO THE CURRENT SPECTRAL SCAN OR
C                COMPLETES THE INITIALIZATION OF SETUP
C                INFORMATION STARTED WITH "NEWSET".
C*********************************************************************
      COMMON/A/NAVG(400),POL(400),ANA(400)
      COMMON/B/NRATE,NSCAN,IPOL,IANA
      COMMON/E/NAMEOP(20),ID(20)
      COMMON/J/NWL,NPOL,NCMP,NANA
      COMMON/K/IHRS0,IMIN0,ISEC0,ITIC0,IHRSF,IMINF,ISECF,ITICF
      COMMON/L/IDAY,IMON(3),IYRS,LMPHRS
      COMMON/O/NPASS
      IF(NPASS.GT.1)GOTO 106
      TYPE 100
  100 FORMAT(/,'$ NAME(A40) = ')
      ACCEPT 101,(NAMEOP(I),I=1,20)
  101 FORMAT(20A2)
      TYPE 102
  102 FORMAT(/,'$ DATE(I2-A3-I2/DAY-MONTH-YEAR) = ')
      ACCEPT 103,IDAY,(IMON(I),I=1,3),IYRS
  103 FORMAT(I2,1X,3A1,1X,I2)
      TYPE 104
  104 FORMAT(/,'$ LAMP OPERATIONAL LIFE(I5/HOURS) = ')
      ACCEPT 105,LMPHRS
  105 FORMAT(I5)
  106 CONTINUE
      TYPE 107
  107 FORMAT(/,'$ EXPERIMENT IDENTIFICATION(A40) = ')
      ACCEPT 101,(ID(I),I=1,20)
        NPOL=9000
        NANA=9000
        NCMP=0
  108 TYPE 109
  109 FORMAT(/,'      INITIAL POSITIONS'
     1,/T5,'POL=90.00',/T5,'ANA=90.00',/T5,'CMP=0.00',/
     2'$',T10,'ANY CHANGES ?')
      ACCEPT 110,MANAZ
  110 FORMAT(A1)
      IF(MANAZ.NE.1HY.AND.MANAZ.NE.1HN)GOTO 108
      IF(MANAZ.NE.1HY)GOTO 119
      TYPE 112
  112 FORMAT(/,' MANUAL AZIMUTH SETTINGS(DEG):')
      TYPE 113
  113 FORMAT('$ POLARIZER(F7.2)    = ')
      ACCEPT 114,P
  114 FORMAT(F7.2)
      NPOL=P*100.
      TYPE 115
  115 FORMAT('$ ANALYZER(F7.2)     = ')
      ACCEPT 114,A
      NANA=A*100.
  116 TYPE 117
  117 FORMAT('$ COMPENSATOR(F7.2) = ')
      ACCEPT 114,C
```

```
      NCMP=C*100.
        TYPE 118
  118 FORMAT('$ MONOCHROMATOR SETTING AT NULL(F7.2) = ')
      ACCEPT 114,WL
      NWL=WL*100.
  119 CONTINUE
      IGAIN=3
      NCHP=0
      NCHA=1
  120 TYPE 121
  121 FORMAT(/,' ANALOG/DIGITAL CONVERTOR PRESET PARAMETERS:')
  122 TYPE 123,NCHP
  123 FORMAT('  POL. INPUT CH. = ',I1)
      TYPE 124,NCHA
  124 FORMAT('  ANA. INPUT CH. = ',I1)
      TYPE 125,IGAIN
  125 FORMAT('  ADC GAIN       = ',I1)
      TYPE 126
  126 FORMAT(/,'$ DO YOU WANT TO CHANGE THESE(Y/N)? ')
      ACCEPT 110,NADC
      IF(NADC.NE.1HY.AND.NADC.NE.1HN)GOTO 120
      IF(NADC.EQ.1HN)GOTO 131
      TYPE 127
  127 FORMAT('$ POL. INPUT CH.(I1) = ')
      ACCEPT 128,NCHP
  128 FORMAT(I1)
      TYPE 129
  129 FORMAT('$ ANA. INPUT CH.(I1) = ')
      ACCEPT 128,NCHA
      TYPE 130
  130 FORMAT('$ ADC GAIN(I1)       = ')
      ACCEPT 128,IGAIN
      GOTO 120
  131 CONTINUE
      IPOL=IGAIN*64+NCHP
      IANA=IGAIN*64+NCHA
      TYPE 132
  132 FORMAT(/,'$ HOW MANY SPECTRAL SCANS ARE TO BE AVERAGED(I5)? ')
      ACCEPT 133,NSCAN
  133 FORMAT(I5)
      DO 140 I=1,400
      POL(I)=0.
      ANA(I)=0.
  140 NAVG(I)=0
      NPASS=NPASS+1
      RETURN
      END
```

```
        subroutine pmt(jk)
D       TYPE *,'PMT'
        jk=0
        do 170 i=1,15
      CALL IPOKE("170400,0)
      CALL IPOKE("170402,6.OR.(0))
1701  IF(.NOT.(IPEEK("170400).AND."100000))GOTO 1701
170     jk=jk+ipeek("170402)
        jk=jk/15
        RETURN
      END

        SUBROUTINE NULL(JPCNT,JACNT,icflg)
D       TYPE *,'NULL'
        COMMON/B/NRATE,NSCAN,IPOL,IANA
        icflg=1
        IGAIN=3
        IPOL=0
        IANA=1
        JPCNT=0
        JACNT=0
        JGAIN=IGAIN*64
        CALL IPOKE("170400,0)
        TYPE 100
        ACCEPT 200,NWAIT
200     FORMAT(I2)
C
C       *******   Null with PMT output   *******
C
        jpflg=0
        idir=2048
        call pmt(i)
        i=-i
D       TYPE *,'1 IF'
        if(i.lt.100)goto 10
11      continue
        i2=i
1001    if(ipeek("164502).gt.0.or.ipeek("164506).gt.0) goto 1001
        CALL IPOKE("164502,50+IDIR)
1002    if(ipeek("164502).gt.0.or.ipeek("164506).gt.0) goto 1002
        jacnt=jacnt-2*idir/2000+1
        call pmt(i)
        i=-i
D       TYPE *,'2 IF'
        if(i.lt.100)goto 10
        if(jacnt.lt.-89)idir=0
        IF(JACNT.EQ.90)GOTO 12
D       TYPE *,'3 IF'
        if(i.le.i2)goto 11
        jpflg=jpflg+1
D       TYPE *,'4 IF'
        if(jpflg.GT.2)goto 12
        idir=0
        goto 11
12      idir=2048
        I3=I
121     i2=i
1003    if(ipeek("164502).gt.0.or.ipeek("164506).gt.0) goto 1003
        CALL IPOKE("164506,50+IDIR)
```

```
1004    if(ipeek("164502).gt.0.or.ipeek("164506).gt.0) goto 1004
        jpcnt=jpcnt+1
        call pmt(i)
        i=-i
D       TYPE *,'5 IF'
        if(i.lt.100)goto 10
D       TYPE *,'6 IF'
        IF(I.GE.I2.AND.I3.GT.I2)GOTO 11
        if(jpcnt.gt.179)goto 13
        I3=I2
        goto 121
13      continue
        print *,'Sorry Sucker !, It didn''t null !'
        icflg=0
        return
c
c       ********  null with polarizer and analyser
c
10      CONTINUE
        IDIR=2048
        JPOL=0
        JANA=0
1000    IF(IPEEK("164502).GT.0.OR.IPEEK("164506).GT.0) GOTO 1000
        DO 750 I=1,15
        CALL IPOKE("170402,IPOL.OR.(JGAIN))
2000    IF(.NOT.(IPEEK("170400).AND."100000)) GOTO 2000
        JPOL=IPEEK("170402)+JPOL
        CALL IPOKE("170402,IANA.OR.(JGAIN))
3000    IF(.NOT.(IPEEK("170400).AND."100000)) GOTO 3000
        JANA=IPEEK("170402)+JANA
750     CONTINUE
        JANA=JANA/15
        JPOL=JPOL/15
        IF(IABS(JPOL).LT.100.AND.IABS(JANA).LT.100) RETURN
        IF(IABS(JPOL).LT.100) GOTO 20
        IF(JPOL.LT.0)IDIR=0.
        IF(JPOL.LT.0)JPCNT=JPCNT-2
        JPCNT=JPCNT+1
        CALL IPOKE("164506,50+IDIR)
        IF(IABS(JANA).LT.100)GOTO 10
        IDIR=2048
20      IF(JANA.GT.0)IDIR=0
        IF(JANA.LT.0)JACNT=JACNT-2
        JACNT=JACNT+1
        CALL IPOKE("164502,50+IDIR)
        GOTO 10
100     FORMAT(T5,'Set monochrometer to prefered wavelenght.',
     *  /T5,'Make sure all necessary intruments are on and',
     *  /T5,'the F.C. controller in closed circut.',
     *  /t5,'Hit return key when ready.')
        END
```

```
      SUBROUTINE T1TIME
C*********************************************************************
C     OBJECTIVE: DISPLAYS THE DATA ACQUISITION TIME FOR THE GIVEN
C                SPECTRAL SCAN ON THE CRT SCREEN.
C*********************************************************************
      COMMON/B/NRATE,NSCAN,IPOL,IANA
      COMMON/K/IHRSO,IMINO,ISECO,ITICO,IHRSF,IMINF,ISECF,ITICF
      TYPE 100,NSCAN
  100 FORMAT(/,10X,'THE NUMBER OF SPECTRA AVERAGED = ',I5)
      TYPE 110,NRATE
  110 FORMAT(10X,'MEASURED SCAN RATE VIA COUNTER = ',I5)
      TYPE 120,IHRSO,IMINO,ISECO,ITICO
  120 FORMAT(/10X,'DATA COLLECTION INITIATED AT: ',3(I2,':'),I2)
      TYPE 130,IHRSF,IMINF,ISECF,ITICF
  130 FORMAT(10X,'DATA COLLECTION FINISHED  AT: ',3(I2,':'),I2)
      RETURN
      END
```

```
      SUBROUTINE T1INFO
C*********************************************************************
C     OBJECTIVE: DISPLAYS ALL THE SETUP INFORMATION FOR A GIVEN
C                SPECTRAL SCAN ON THE VT55 GRAPHICS TERMINAL SCREEN,
C                EXCEPT FOR THE DATA ACQUISTION TIME.
C*********************************************************************
      COMMON/B/NRATE,NSCAN,IPOL,IANA
      COMMON/E/NAMEOP(20),ID(20)
      COMMON/F/LMPTYP,LMPSER(10),LMPVLT,LMPAMP
      COMMON/G/IPMTYP(10),IPMTDV
      COMMON/H/IPHASP,IPHASA,IGAINP,IGAINA,IAMPLP,IAMPLA,ITIMEP,ITIMEA
      COMMON/I/IGAGP,IGAGA,IGATP,IGATA
      COMMON/J/NWL,NPOL,NCMP,NANA
      COMMON/K/IHRS0,IMIN0,ISEC0,ITIC0,IHRSF,IMINF,ISECF,ITICF
      COMMON/L/IDAY,IMON(3),IYRS,LMPHRS
      TYPE 100,IDAY,(IMON(I),I=1,3),IYRS
  100 FORMAT(/10X,I2,'-',3A1,'-',I2)
      TYPE 101,(NAMEOP(I),I=1,20)
  101 FORMAT(10X,10A2)
      TYPE 102,(ID(I),I=1,20)
  102 FORMAT(10X,20A2)
      TYPE 110
  110 FORMAT(/10X,'MANUAL AZIMUTHS(DEG):')
      P=NPOL/100.
      A=NANA/100.
      C=NCMP/100.
      WL=NWL/100.
      TYPE 111,P,A,C,WL
  111 FORMAT(/12X,'P = ',F7.2,
     C        /12X,'A = ',F7.2,
     C        /12X,'C = ',F7.2,
     C        /12X,'WL= ',F7.2)
      TYPE 120
  120 FORMAT(/10X,'LAMP:')
      TYPE 121,LMPTYP
  121 FORMAT(/12X,'TYPE        = ',A2)
      TYPE 122,(LMPSER(I),I=1,9)
  122 FORMAT(12X,'SERIAL NO. = ',9A2)
      TYPE 123,LMPVLT
  123 FORMAT(12X,'LAMP VOLTAGE(VOLTS) = ',I4)
      TYPE 124,LMPAMP
  124 FORMAT(12X,'LAMP CURRENT(AMPS)  = ',I3)
      TYPE 125,LMPHRS
  125 FORMAT(12X,'LAMP OPERATIONAL LIFE(HOURS) = ',I5)
      TYPE 130
  130 FORMAT(/10X,'PHOTOMULTIPLIER:')
      TYPE 131,(IPMTYP(I),I=1,10)
  131 FORMAT(/12X,'MODEL = ',10A2)
      TYPE 132,IPMTDV
  132 FORMAT(12X,'DYNODE VOLTAGE(VOLTS) = ',I5)
      TYPE 140
  140 FORMAT(/10X,'FARADAY CELL CONTROLLER:')
      TYPE 141
  141 FORMAT(/12X,'POLARIZER')
      TYPE 142,IPHASP,IGAINP,IAMPLP,ITIMEP
  142 FORMAT(/12X,'PHASE              = ',I4,
     C        /12X,'GAIN               = ',I4,
     C        /12X,'AMPLITUDE          = ',I4,
     C        /12X,'TIME CONSTANT(MS) = ',I4)
```

```
      TYPE 143
  143 FORMAT(/12X,'ANALYZER')
      TYPE 142,IPHASA,IGAINA,IAMPLA,ITIME
      TYPE 150
  150 FORMAT(/10X,'GALVANOMETER AMPLIFIEI
      TYPE 141
      TYPE 151,IGAGP,IGATP
  151 FORMAT(/12X,'GAIN                 = '
     C        /12X,'TIME CONSTANT(MS) = '
      TYPE 143
      TYPE 151,IGAGA,IGATA
      IGAIN=IPOL/64
      NCHP=IPOL-IGAIN*64
      NCHA=IANA-IGAIN*64
      TYPE 160
  160 FORMAT(/10X,'ANALOG/DIGITAL CONVEI
      TYPE 161,NCHP,NCHA,IGAIN
  161 FORMAT(/12X,'POL. INPUT CH. = ',I
     C        /12X,'ANA. INPUT CH. = ',I
     C        /12X,'ADC GAIN       = ',I
      RETURN
      END
```

```
      SUBROUTINE P1INFO
C*********************************************************************
C     OBJECTIVE: OUTPUTS ALL THE SETUP INFORMATION FOR A SPECTRAL SCAN
C                TO THE LINE PRINTER, EXCEPT FOR THE DATA ACQUISITION
C                TIME.
C*********************************************************************
      COMMON/B/NRATE,NSCAN,IPOL,IANA
      COMMON/E/NAMEOP(20),ID(20)
      COMMON/F/LMPTYP,LMPSER(10),LMPVLT,LMPAMP
      COMMON/G/IPMTYP(10),IPMTDV
      COMMON/H/IPHASP,IPHASA,IGAINP,IGAINA,IAMPLP,IAMPLA,ITIMEP,ITIMEA
      COMMON/I/IGAGP,IGAGA,IGATP,IGATA
      COMMON/J/NWL,NPOL,NCMP,NANA
      COMMON/K/IHRSO,IMINO,ISECO,ITICO,IHRSF,IMINF,ISECF,ITICF
      COMMON/L/IDAY,IMON(3),IYRS,LMPHRS
      PRINT 100,IDAY,(IMON(I),I=1,3),IYRS
  100 FORMAT(/10X,I2,'-',3A1,'-',I2)
      PRINT 101,(NAMEOP(I),I=1,20)
  101 FORMAT(10X,20A2)
      PRINT 102,(ID(I),I=1,20)
  102 FORMAT(10X,20A2)
      PRINT 110
  110 FORMAT(/10X,'MANUAL AZIMUTHS(DEG):')
      P=NPOL/100.
      A=NANA/100.
      C=NCMP/100.
      WL=NWL/100.
      PRINT 111,P,A,C,WL
  111 FORMAT(/12X,'P = ',F7.2,
     C        /12X,'A = ',F7.2,
     C        /12X,'C = ',F7.2,
     C        /12X,'WL= ',F7.2)
      PRINT 120
  120 FORMAT(/10X,'LAMP:')
      PRINT 121,LMPTYP
  121 FORMAT(/12X,'TYPE        = ',A2)
      PRINT 122,(LMPSER(I),I=1,9)
  122 FORMAT(12X,'SERIAL NO. = ',9A2)
      PRINT 123,LMPVLT
  123 FORMAT(12X,'LAMP VOLTAGE(VOLTS) = ',I4)
      PRINT 124,LMPAMP
  124 FORMAT(12X,'LAMP CURRENT(AMPS)  = ',I3)
      PRINT 125,LMPHRS
  125 FORMAT(12X,'LAMP OPERATIONAL LIFE(HOURS) = ',I5)
      PRINT 130
  130 FORMAT(/10X,'PHOTOMULTIPLIER:')
      PRINT 131,(IPMTYP(I),I=1,10)
  131 FORMAT(/12X,'MODEL = ',10A2)
      PRINT 132,IPMTDV
  132 FORMAT(12X,'DYNODE VOLTAGE(VOLTS) = ',I5)
      PRINT 140
  140 FORMAT(/10X,'FARADAY CELL CONTROLLER:')
      PRINT 141
  141 FORMAT(/12X,'POLARIZER')
      PRINT 142,IPHASP,IGAINP,IAMPLP,ITIMEP
  142 FORMAT(/12X,'PHASE              = ',I4,
     C        /12X,'GAIN               = ',I4,
     C        /12X,'AMPLITUDE          = ',I4,
     C        /12X,'TIME CONSTANT(MS)  = ',I4)
```

```
      PRINT 143
  143 FORMAT(/12X,'ANALYZER')
      PRINT 142,IPHASA,IGAINA,IAMPLA,ITIMEA
      PRINT 150
  150 FORMAT(/10X,'GALVANOMETER AMPLIFIER:')
      PRINT 141
      PRINT 151,IGAGP,IGATP
  151 FORMAT(/12X,'GAIN                 = ',I6,
     C       /12X,'TIME CONSTANT(MS) = ',I6)
      PRINT 143
      PRINT 151,IGAGA,IGATA
      IGAIN=IPOL/64
      NCHP=IPOL-IGAIN*64
      NCHA=IANA-IGAIN*64
      PRINT 160
  160 FORMAT(/10X,'ANALOG/DIGITAL CONVERTOR:')
      PRINT 161,NCHP,NCHA,IGAIN
  161 FORMAT(/12X,'POL. INPUT CH. = ',I1,
     C       /12X,'ANA. INPUT CH. = ',I1,
     C       /12X,'ADC GAIN       = ',I1)
      RETURN
      END
```

```
      SUBROUTINE PITIME
C*********************************************************************
C     OBJECTIVE: OUTPUTS THE DATA ACQUISITION FOR THE GIVEN SPECTRAL
C                SCAN TO THE LINE PRINTER.
C*********************************************************************
      COMMON/B/NRATE,NSCAN,IPOL,IANA
      COMMON/K/IHRSO,IMINO,ISECO,ITICO,IHRSF,IMINF,ISECF,ITICF
      PRINT 100,NSCAN
  100 FORMAT(/,10X,'THE NUMBER OF SPECTRA AVERAGED = ',I5)
      PRINT 110,NRATE
  110 FORMAT(10X,'MEASURED SCAN RATE VIA COUNTER = ',I5)
      PRINT 120,IHRSO,IMINO,ISECO,ITICO
  120 FORMAT(/10X,'DATA COLLECTION INITIATED AT: ',3(I2,':'),I2)
      PRINT 130,IHRSF,IMINF,ISECF,ITICF
  130 FORMAT(10X,'DATA COLLECTION FINISHED  AT: ',3(I2,':'),I2)
      RETURN
      END
```

```
      SUBROUTINE WLCALC
C*********************************************************************
C     OBJECTIVE: TO CONVERT ENCODER COUNTS INTO WAVELENGTH USING
C                PREDETERMINED CALIBRATION CURVE PARAMETERS.
C*********************************************************************
      COMMON/M/IWAVE(400)
      OPEN(UNIT=2,NAME='DY1:WLCALC.DAT',TYPE='OLD')
      READ(2,996)IU,IL,A1,B1,R1,A2,B2,R2
  996 FORMAT(2(1X,I3),2(1X,F8.4,1X,F8.2,1X,F6.4))
      CLOSE(UNIT=2,DISPOSE='SAVE')
  997 TYPE 998
  998 FORMAT(/,'$ DO YOU WANT TO REVIEW ENCODER WAVELENGTH CALIBRATION
     C PARAMETERS(Y/N)? ')
      ACCEPT 999,IF0
      IF(IF0.NE.1HY.AND.IF0.NE.1HN)GOTO 997
      IF(IF0.EQ.1HN)GOTO 3
  999 FORMAT(A1)
      TYPE 1000
 1000 FORMAT(//,10X,'DIGITAL ENCODER PRESETS:')
    1 TYPE 1001,A1,B1,R1
 1001 FORMAT(/,10X,'CALIBRATION CURVE SEGMENT NUMBER 1:',
     C       /,15X,'SLOPE = ',F10.4,
     C       /,15X,'INTERCEPT = ',F10.2,
     C       /,15X,'CORRELATION COEFFICIENT = ',F10.4)
      TYPE 1002,A2,B2,R2
 1002 FORMAT(/,10X,'CALIBRATION CURVE SEGMENT NUMBER 2:',
     C       /,15X,'SLOPE = ',F10.4,
     C       /,15X,'INTERCEPT = ',F10.2,
     C       /,15X,'CORRELATION COEFFICIENT = ',F10.4)
      TYPE 1003,IL,IU
 1003 FORMAT(/,10X,'LIMITS OF APPLICATION:',
     C       /,15X,'UPPER = ',I6,
     C       /,15X,'LOWER = ',I6)
    2 TYPE 1004
 1004 FORMAT(/,'$ DO YOU WANT TO CHANGE THESE(Y/N)? ')
      ACCEPT 1005,IF1
 1005 FORMAT(A1)
      IF(IF1.NE.1HY.AND.IF1.NE.1HN)GOTO 2
      IF(IF1.EQ.1HN)GOTO 3
      TYPE 1006
 1006 FORMAT(/,2X,'SEGMENT 1:')
      TYPE 1007
 1007 FORMAT(/,'$ SLOPE(F10.4/ANGSTROMS PER COUNT) = ')
      ACCEPT 1008,A1
 1008 FORMAT(F10.4)
      TYPE 1009
 1009 FORMAT(/,'$ INTERCEPT(F10.2/ANGSTROMS)       = ')
      ACCEPT 1010,B1
 1010 FORMAT(F10.2)
      TYPE 1011
 1011 FORMAT(/,'$ CORRELATION COEFFICIENT(F10.4)   = ')
      ACCEPT 1012,R1
 1012 FORMAT(F10.4)
      TYPE 1013
 1013 FORMAT(/,2X,'SEGMENT 2:')
      TYPE 1007
      ACCEPT 1008,A2
      TYPE 1009
      ACCEPT 1010,B2
```

```
      TYPE 1011
      ACCEPT 1012,R2
      TYPE 1014
 1014 FORMAT(/,'$ UPPER LIMIT OF APPLICATION(I6) = ')
      ACCEPT 1015,IL
 1015 FORMAT(I6)
      TYPE 1016
 1016 FORMAT(/,'$ LOWER LIMIT OF APPLICATION(I6) = ')
      ACCEPT 1015,IU
      GOTO 1
    3 CONTINUE
      DO 40 I=1,400
      IF(I.LE.IL.AND.I.GE.IU)GOTO 10
      IF(I.GT.IL)GOTO 20
      COUNT=I
      WL=A1*COUNT+B1
      GOTO 30
   10 COUNT=I
      WL=A2*COUNT+B2
      GOTO 30
   20 COUNT=I-400
      WL=A1*COUNT+B1
   30 CONTINUE
   40 IWAVE(I)=WL
      RETURN
      END
```

9. References

1) J.C. Farmer with R.H. Muller, "Effect of Organic Adsorbates on the Initial Stage of Electrolytic Metal Deposition: Development and Use of a Spectroscopic Ellipsometer," PhD thesis, U. Calif. Berkeley, 1983, LBL-15607

2) R.H. Muller and J.C. Farmer, Surf. Sci., 135, 521-531 (1983)

3) M.P. Seah and C.P. Hunt, Surf. Interface Anal., 5, 33 (1983)

4) G. K. Wehner, "The Aspects of Sputtering in Surface Analysis Methods," METHODS OF SURFACE ANALYSIS, A.W. Czanderna ed., Elsevier Co., (1975) p 9

5) G.K. Wehner and D.J. Hajicek, J. Appl. Phys., 42, 1145-1149 (1971)

6) M.L. Tarng and G.K. Wehner, J. Appl. Phys., 43, 2268 (1972)

7) R. Kelly and O. Auciello, Surf. Sci., 100, 135 (1980)

8) G.W. Lewis, G. Kiriakides, G. Carter, and M.J. Nobes, Surf. Interface Anal., 4, 141 (1982)

9) H. Yasuda and K. Nagai, Jap. J. Appl. Phys., 11, 1723-1716 (1972)

10) P. H. Holloway and S. K. Hofmeister, Surf. Interface Anal., 4, 181 (1982)

11) M.A. Burke and J.J. Schreurs, Surf. Interface Anal., 5, 155 (1983)

12) N.J. Chou and M.W. Shafer, Surf. Sci., 92, 601 (1980)

13) Ion Beam Etch Rates, Bulletin 137-78, Commonwealth Scientific Corp., Virgina, 1978.

14) D.K. Skinner, J.G. Swanson, and C.V. Haynes, Surf. Interface Anal., 5, 38 (1983)

15) H.H. Anderson, Appl. Phys., 18, 131 (1979)

16) D.E. Aspnes and A.A. Studna, Surf. Sci., 96, 294 (1980)

17) M.M. Ibrahim and N.M. Bashara, Surf. Sci., 30, 632 (1972)

18) P.W. Palmberg, J. Appl. Phys., 38, 2137-2147 (1967)

19) R.E. Weber and W.T. Peria, J. Appl. Phys., 38, 4355-4358 (1967)

20) R.H. Muller and J.C. Farmer, Rev. Sci. Instrum., 55, 371-374 (1984)

21) H.J. Mathieu, D.E. McClure, and R.H. Muller, Rev. Sci. Instrum., 45, 798 (1974)

22) R.H. Muller, "PRINCIPLES OF ELLIPSOMETRY," ADVANCES IN ELECTROCHEMISTRY, vol. 9, P. Delahay, C.W. Tobias eds., Wiley, New York, 1973, pp. 167-226

23) C.G. Grandquvist and O. Hunderi, Phys. Rev., B 16, 3513 (1977)

24) D.E. Aspnes, E. Kinsbron, and D.D. Bacon, Phys. Rev., B 21, 3290 (1980)

25) D.E. Aspnes and J.B. Theeten, Phys. Rev., B 20, 3292 (1979)

26) O. Hunderi, Surf. Sci., 96, 1 (1980)

27) M. Born and E. Wolf, Principles of Optics, MacMillan, New York, 1964, p 551

28) J.C. Farmer with R.H. Muller, "Automatic etc.," Univ. of Calif., Berkeley, (1983) LBL-15525

29) P.B. Johson and R.W. Christy, Phys. Rev., B 6, 4370 (1972)

30) G. Hass and L. Hadley, Optical Properties of Metals, in: American Institute of Physics Handbook, 2nd ed., D.E. Gray eds. (McGraw-Hill, New York, 1963) p. 6-103

31) A. Joshi, L.E. Davis, and P.W. Palmberg, "Auger Electron Spectroscopy," Ch. 5 in METHODS OF SURFACE ANALYSIS, A.W. Czanderna, ed., (1975) pp 159-194

32) P.W. Palmberg, G.E. Riach, R.E. Weber, and N.C. MacDonald, HANDBOOK OF AUGER ELECTRON SPECTROSCOPY, Physical Electronics Industries, Edina, 1972.

33) Y.E. Strausser, J.J. Uebbing, Varian Chart of Auger Electron Energies, Varian Vac. Div., 1971

34) R.M.A. Azzam and N.M. Bashara, ELLIPSOMETRY AND POLARIZED LIGHT, North Holland, (1979) p 175

35) V. Alexander, Radiat. Eff., 56, 241-250 (1981)

36) H.G. Liljenvall, A.G. Mathewson, and H.P. Meyers, Phil. Mag., 22, 243, (1970)

This report was done with support from the Department of Energy. Any conclusions or opinions expressed in this report represent solely those of the author(s) and not necessarily those of The Regents of the University of California, the Lawrence Berkeley Laboratory or the Department of Energy.

Reference to a company or product name does not imply approval or recommendation of the product by the University of California or the U.S. Department of Energy to the exclusion of others that may be suitable.

TECHNICAL INFORMATION DEPARTMENT
LAWRENCE BERKELEY LABORATORY
UNIVERSITY OF CALIFORNIA
BERKELEY, CALIFORNIA 94720